NASA TM-83203

NASA Technical Memorandum 83203

NASA-TM-83203 19820002247

MASS LOSS OF TEOS-COATED RCC SUBJECTED TO THE ENVIRONMENT AT THE SHUTTLE WING LEADING EDGE

C. W. Stroud and Donald R. Rummler

SEPTEMBER 1981

National Aeronautics and Space Administration

Langley Research Center
Hampton, Virginia 23665

ABSTRACT

Coated, reinforced carbon-carbon (RCC) is used for the leading edges of the Space Shuttle. The mass loss characteristics of RCC specimens coated with tetra-ethyl-ortho-silicate (TEOS) were determined for conditions which simulated the entry environment expected at the stagnation area of the wing leading edge. Maximum specimen temperature was 1632 K. Specimens were exposed for up to 100 missions. Stress levels up to 8.274 MPa caused an average increase in oxidation of 6 percent over unstressed specimens. Experimentally determined mass losses were compared with those predicted by an existing empirical analysis.

SUMMARY

Reinforced carbon-carbon (RCC) is used as a thermal protection system for the leading edges of the Space Shuttle. The baseline material is coated with tetra-ethyl-ortho-silicate (TEOS) for additional oxidation resistance and is then designated as TEOS-coated RCC. In the present investigation TEOS-coated RCC specimens were exposed to the simultaneous application of load, temperature and oxygen partial pressure to simulate the Shuttle entry environment. The mass loss characteristics of TEOS-coated RCC specimens were determined for conditions which simulated the entry environment expected at the stagnation area of the wing leading edge. Maximum specimen temperature was 1632 K. Specimens were exposed for up to 100

Stress levels up to 8.174 MPa caused an average increase in oxidation rate of 6 percent over unstressed specimens. Experimentally determined mass losses were compared with those predicted by an existing empirical analysis.

INTRODUCTION

The thermal protection system for the wing leading edge and nose cap of the Space Shuttle is constructed of a reinforced carbon-carbon material (RCC). RCC is a laminated carbon-carbon substrate with an oxidation-resistant coating. In spite of the coating, RCC was found to undergo moderate oxidation at temperatures and oxygen partial pressures typical of Shuttle entry. Consequently, methods for further improvements in oxidation protection for RCC were investigated (refs. 1-5). These efforts concentrated on the development of a second coating that could be applied over the baseline coating. A second coating that was light weight and had superior oxidation resistance in certain ranges of temperature and oxygen partial pressure was developed in 1976 by Vought Corporation. Tetra-ethyl-ortho-silicate (TEOS) is applied to the coated part using a vacuum impregnation process, and the material with this second coating is designated TEOS-coated RCC.

The present investigation is a continuation of work reported in reference 6. The first objective of the present investigation was to obtain mass loss data for TEOS-coated RCC under conditions of simultaneous application of the temperatures, oxygen partial pressure and stresses expected

along the stagnation line of the Shuttle wing leading edge during a nominal entry. The second objective was to determine whether the externally applied stress had a significant effect on the mass loss of TEOS-coated RCC under the simulated entry conditions. Both objectives were achieved by subjecting TEOS-coated RCC specimens to an environment which simulated flight-by-flight entry conditions along the stagnation region of the Shuttle wing leading edge. The inside surface of the wing leading edge, along the stagnation line, was selected because expected temperatures during entry are higher there than at any other point on the wing leading edge segments (1632 K). The wing location simulated in these tests was at 55 percent half-span where extensive thermo-structural analyses had previously been performed. A complete factorial experiment was carried out with stress at two levels (zero and expected operational stress). The factorial experiment was designed to achieve the second objective. A required sub-set of the factorial experiment generated the data necessary to achieve the first objective.

SYMBOLS

The units used for the physical quantities defined in this section are given in the International System of Units (SI) (ref. 7). The measurements and calculations were made in U.S. Customary Units.

A_p	calculated area, m^2
B	mass loss constant
d	diameter, m
E_i	activation energy, J/mole
$F_\alpha(v_1,v_2)$	ratio of variances of two independent random samples
K_i	mass loss rate constant
ℓ	length , m
m	mass loss, kg/m^2
m_L	accumulated mass loss, kg/m^2
$\dot{m}$	mass loss rate, kg/m^2 -sec
n	pressure exponent
P	pressure, pa (atm)
R	gas constant, 8.3143 J/mole-K
r_i	shoulder radius, m
T	temperature, K
t_i	thickness, m
t_w	weighted thickness, m
V_b	bulk volume, m^3
v_1	degrees of freedom for the sample variance of the numerator
v_2	degrees of freedom for the sample variance of th denominator
w_i	width, m
ρ	bulk density, kg/m^3

Subscripts:

i	integer
n	number of missions
α	upper probability level

TEST SPECIMENS

Nine RCC mass-loss specimens were cut from a sheet of 19-ply material according to the specimen layout shown in figure 1. The sheet material is a laminate made from a phenolic pre-pregged, square-weave graphite-cloth fabric pyrolyzed to the carbon state. The pyrolyzed substrate was subjected to three furfuryl alcohol impregnations, each followed by pyrolysis to improve density and strength. After being cut from the sheet, the specimens were machined to size. Next, the baseline oxidation-resistant coating was applied to each specimen by packing the composite in a powder composed by weight of 60 percent silicon carbide, 10 percent aluminum oxide, and 30 percent silicon. The packed specimens were then heated to a high temperature in an inert atmosphere. The TEOS coating was subsequently applied on each specimen using a vacuum impregnation process. The impregnated specimens were then cured at 363 K. The impregnation process was repeated five times before the final curing process at 590 K for 3.5 hours. The coating produced by this process is composed of small amorphous silica particles. Photographs of a typical as-received specimen are shown in figure 2.

The nominal dimensions of the TEOS-coated RCC specimens are shown in figure 3. The method used to determine actual specimen dimensions is given in Appendix A. Table I presents the results of measurements to determine the actual dimensions of each specimen. Table II presents other physical characteristics of the TEOS-coated RCC specimens such as as-received mass, mass before drying, mass after drying, calculated bulk volume, bulk density, calculated surface area, effective cross sectional area, and weighted thickness (as defined in Appendix A).

EQUIPMENT AND PROCEDURES

Multiparameter Test System

All tests in this study were performed in a multiparameter test system at the Langley Research Center. A block diagram and a photograph of this system are shown in figure 4. The system consists of three vacuum furnaces, analog controls, and computer complex. Each vacuum furnace has the capability of independently loading six thin-sheet tensile specimens simultaneously. Cylindrical clamshell heating elements surround all six loading locations in each vacuum furnace. The heated zone of the furnaces is 15 cm in diameter and 30 cm long. Each of the three vacuum furnaces can be controlled continuously over a pressure range of 1.33 mPa to 101.3 kPa. The three control parameters - specimen load, temperature, and chamber pressure - are each controlled by the analog closed-loop servo system. A process-con-

trol computer provides the control signals for each vacuum chamber for the desired parameter history and also monitors system responses such as temperature, specimen load, and chamber pressure. Digital-to-analog (D/A) and analog-to-digital (A/D) converters provide communication links between the computer and vacuum furnaces.

For the current test series, only one vacuum chamber was used. The chamber had previously been modified to test three thick (up to 10 mm) specimens simultaneously. The modification was necessary to provide clearance between the thick specimens and the heating elements. The configuration of the modified loading system is shown schematically in figure 5. During a test, the two specimens were mounted in locations A and B. A silicon carbide block was mounted in the third position. The control thermocouple and a backup thermocouple were bonded to the block. The block was clamped in place and never allowed to move during calibration or testing. Also shown is the inlet air distribution manifold. This manifold directs air onto the test specimens surface to assure purging of that area of combustion products. A vacuum pump draws gas through the carbon dioxide monitoring tube to a carbon dioxide analyzer, thus verifying that an oxidizing atmosphere is present at all times. During this test series, the CO_2 concentration never exceeded 0.6% by volume. Figure 6 gives a detailed sketch of the load train and shows the location of thermocouples in a TEOS-coated calibration specimen which was used to determine temperature distributions during system calibration.

Testing Procedures

The nominal test specimen temperature, stress level and chamber air pressure histories are presented in figure 7. The histories in figure 7 were generated using the values listed in Table III with linear interpolation between points of temperature and stress, and logarithmic interpolation between points of pressure. These histories indicate environmental conditions in the stagnation region of the wing leading edge at 55 percent half-span of the Shuttle during entry. The desired tolerance for the three controlled variables with respect to nominal profiles were as follows:

Temperature: $\pm$16.7 K

Air Pressure: $\pm$267 Pa for $0 < P < 13.3$ kPa

$\pm$666 Pa for $13.3 < P \leq 101.3$ kPa

Stress: $\pm$ 5 percent or $\pm$ 170 kPa, whichever is greater

An additional requirement was that the dew point of the inlet air be less than 230 K to simulate the relatively dry air encountered during reentry and minimize the catalytic effects of moisture on the oxidation of carbon.

Achieving the desired tolerance in temperature was difficult. A discussion of the calibration procedure and final results is summarized in Appendix B.

Calibration mission mass losses were calculated using the empirical prediction equation in Appendix C and actual calibration temperatures and chamber pressures. These mass losses were compared with those defined by the nominal Shuttle mission plus or minus the nominal tolerances on temperature and pressure defined above. The comparison of these mass losses demonstrated that:

1. The calibration mission mass losses for all points on the specimen are well within nominmal mission mass loss tolerance bounds.
2. The reproducibility from one mission to the next is excellent.

Facility calibration indicated that sample location in the furnace could be a significant source of experimental variability. For this reason, sample location was randomized as much as possible by changing the location (A or B) in the furnace of the loaded specimen each time a new set of specimens was tested. Since two specimens were tested at a time, one was loaded to the mission profile and the other kept under a constant small stress of less than 170 kPa (hereinafter referred to as the no-load condition). The specimens were tested in pairs as follows:

Test Series	Specimen Number	Load Condition	Furnace Location
I	1	No Load	A
(50 missions)	2	Load	B
II	5	No Load	B
(100 missions)	3	Load	A
III	8	No Load	A
(100 Missions)	7	Load	B
IV	6	No Load	B
(50 missions)	4	Load	A

To minimize contamination, the specimens were handled with new white cotton gloves each time they were removed from the test chamber. The order in which the specimens were removed from the test chamber, weighed, and photographed was alternated each time the specimens were removed (five-mission intervals). The specimens were stored in a dessicator except when they were in the test chamber or when they were being photographed and weighed. This procedure minimized the transport of oxygen to the interior of the specimen by moisture absorption.

The simulated missions were monitored with an on-line plotter which displayed the differences between the command and the response of the three controlled parameters. An on-line printer

provided a hard copy of parameter values at six second intervals. Data were recorded on tape at six-second intervals and used for subsequent analysis.

RESULTS AND DISCUSSION

Mass-Loss Data

The mass loss data for eight specimens are tabulated in Table IV (specimen 9 was used for temperature control). The mass loss per unit surface area is listed after five mission intervals . The mass loss was obtained as follows:

$$\text{Mass loss} = \frac{\text{Initial dry weight - current weight}}{\text{Surface area}} \qquad (1)$$

All values of mass loss in the following discussions are based on mass loss per unit surface area. Specimens 1 and 2 and specimens 4 and 6 were tested in pairs for 50 missions. Specimens 3 and 5 and specimens 7 and 8 were tested in pairs until the mass loss of one of the pairs exceeded 488 g/m^2 or 100 missions. Both pairs of specimens reached 100 missions before any specimen had a mass loss greater than 488 g/m^2. A plot of the mass loss of each specimen is shown in figure 8. Also shown is the empirical mass loss prediction computed using actual temperatures and pressures. These computations used the Vought Corporation mass loss prediction equation presented in Appendix C. Rapid mass loss occurs during the first mission as is shown

in test series I where the specimen was removed and weighed after one mission. A volatile component is apparently being released by the high temperatures in the test profile. After these volatiles are removed, the mass loss was continuous with an increasing slope. If the volatiles are excluded, the calculated mass loss is greater than the observed mass loss in every case.

This is in contrast to previous cyclic mass loss testing on this material (ref. 6) where excellent agreement between the calculated and observed mass loss was obtained. The simulation cycle for the current tests include all three of the oxidation control regimes proposed in reference 3: the low temperature reaction controlled regime, the intermediate temperature transition regime, and the high temperature diffusion controlled regime. Previous cyclic mass loss testing (ref. 6) was within the reaction controlled regime (maximum specimen temperature $\leq$900 K). The lack of agreement between calculated and observed mass losses shown in figure 8 suggests that the Vought prediction equation overpredicts observed mass loss for the transition and/or diffusion controlled regimes.

Photographs of specimen 7 after 100 missions are shown in figure 9. This specimen was typical of all specimens tested. There was a glazing of the surface as a result of exposure to the high temperature.

Analysis of Variance of Mass Loss

One of the major objectives of this study was to determine whether the simultaneous application of load, temperature, and oxygen partial pressure to the TEOS-coated material caused higher mass loss than when only temperature and pressure were applied. In addition to the load parameter, an additional variable of furnace location was inherent in the test results. Two furnace locations, A and B, were used to reduce the testing time, and as indicated in previous studies (ref 6), mass loss was affected by furnace location. Thus, two levels of load and two furnace locations were considered. To resolve these effects, the testing was carried out as a complete factorial experiment. The mass-loss results after 50 missions are shown in the following table:

Factor 1: Furnace Location	Factor 2: Load or No Load	Replication 1 Mass loss, g/m^2	Replication 2 Mass loss, g/m^2
A	Load	31.64	33.34
B	No Load	28.85	30.27
A	No Load	30.27	30.02
B	Load	30.22	31.24
TOTAL		120.98	124.87

An analysis of variance was performed (in accordance with ref. 8) on the above data with the following results:

Source of Variance	Degrees of Freedom	Sum of Squares	Mean Squares	F
Main effects:				
Load	1	.2592	.2592	8.19
Location	1	.1152	.1152	3.64
Interaction	1	.0288	.0288	0.91
Error	4	.1266	.03165	
Total	7	.5298		

The values of F show that the load is significant at the 95-percent confidence level. That is, F value for load exceeded the $F_{.05}$ (1, 4) value of 7.71. After 50 missions, the average mass loss of the loaded specimens exceeded the average mass loss of the "No load" specimens by 6%. The above analysis of variance shows that this difference is statistically significant. No other factors were significant at the 95 percent confidence level.

Effects of RCC Bulk Density on Mass Loss

Previous tests of the lug area of the leading edge have shown that overall mass loss could be correlated with bulk density of the TEOS-coated RCC material (ref. 6). In that study, a linear least squares curve fit was made to the mass loss data and the following equation was obtained:

$$M_{50} = 9321.5 - 5598\ \rho \qquad (2)$$

where ρ is the initial bulk density in gm/cm^3, and M_{50} is the predicted mass loss after 50 missions, in gm/m^2.

An attempt was made to correlate the mass loss data obtained for the stagnation point in the present study. In figure 10, the mass loss after 50 missions is plotted as a function of calculated initial bulk density. No trend is apparent.

CONCLUDING REMARKS

The two major objectives for this study of TEOS-coated RCC have been achieved. First, consistent mass loss data were obtained from specimens which were simultaneously exposed to the temperatures, oxygen partial pressures and stresses to simulate expected conditions along the stagnation line of the Shuttle wing leading edge during a nominal entry. In contrast to previous mission simulation testing where the maximum cycle temperature was 900 K, predicted and observed mass loss were not in good agreement for these simulation tests where the maximum cycle temperature was 1632 K. The lack of agreement between predicted and observed mass loss for the high temperature mission cycles suggests that the mass loss prediction equation overpredicts mass loss for the transition and/or diffusion controlled oxidation regimes. Also, in contrast to the previous low temperature simulation testing, no correlation was found between specimen bulk density and observed mass loss.

Second, stress levels of 8.3 MPa moderately increased the mass loss of the TEOS-coated RCC specimens. The average mass

loss of stressed specimens exceeded the average mass loss of unstressed specimens by approximately 6 percent. This is also in contrast to the previous low temperature mission simulation tests where no effect of stress on mass loss was observed for stress levels up to 6.8 MPa.

APPENDIX A

MEASUREMENT OF TEOS-COATED RCC SPECIMENS

To determine both surface area and bulk volume, the dimensions shown in figure 11 were determined. The linear measurements were made with flat anvil micrometers. Shoulder radius measurements, $r_{1,2,3,4}$, were made by comparison with 72.4 mm, 73.7 mm, and 74.9 mm radius blocks. The radii were determined to be 73.7 mm for all specimens. To preclude coating damage, the diameters of the two pull holes were not measured. All pull holes were assumed to have the nominal dimensions (diameter = 12.7 mm). The dimensions of all specimens are shown in Table I.

The specimens were weighed in the as-received condition and after drying overnight in a vacuum at a temperature of 396 K in the multiparameter test system. The results of these measurements are presented in Table II, along with the calculated values for bulk volume, bulk density surface area, effective cross-sectional area and weighted thickness.

Bulk volume was computed using a calculated planform area and an average thickness that was weighted with respect to the area between thickness measurements:

$$V_b = A_p \, t_w \qquad \text{(A-1)}$$

where

A_p calculated planform area, cm^2

V_b bulk volume, cm^3

$$t_w = A_1 \frac{(t_1 + t_2)}{2} + A_2 \frac{(t_2 + t_3 + t_4)}{3} + A_3 \frac{(t_4 + t_5)]}{2} \qquad (A\text{-}2)$$

$A_1 = A_3 = 7/16$

$A_2 = 1/8$

t_i thickness, cm

APPENDIX B

SYSTEM PREPARATION DETAILS

The results of previous testing and preliminary oxidation testing confirmed that the multiparameter test system provided adequate airflow at all temperatures and pressures to prevent a buildup of oxidation products which could shield TEOS-coated RCC materials from an oxidizing environment. These tests, run with both graphite and RCC coupons, established the following:

1. The vacuum pumping system provides approximately 10 times the airflow necessary to maintain the free oxygen content in the chamber at a level at least 95 percent of normal atmospheric concentration if no more than three TEOS-coated RCC specimens are tested simultaneously.

   Test results with graphite coupons showed that the CO_2 in the affluent gas never exceeded two percent. Initially, carbon monoxide was also monitored. Monitoring of carbon monoxide was discontinued when the levels were found to be consistently <2 ppm.

2. The air dryer installed in the system for the TEOS-coated RCC tests was adequate to meet the dew point requirements. The dew point of the chamber inlet air was measured with an electrolytic hygrometer. Constant

monitoring over a period of weeks showed that the dew point of the dried air was always less than 218 K. These determinations were made at flow rates approximately four times maximum vacuum pump capabilities or about 40 times the anticipated maximum flow requirements. Thus, dew points in the chamber were significantly lower than 218 K during the tests.

Temperature Calibration

The objective of the temperature calibration was to control temperature at all points on the specimen to within 16.7 K of the nominal Shuttle profile.

Previous experience with specimens of this type indicated that directly measuring the temperature of TEOS-coated RCC specimens was extremely difficult. Reproducible temperature measurements were not obtained until platinum/platinum-13% rhodium thermocouples were embedded in a specimen. Embedding thermocouples in each specimen was not feasible since the procedure would destroy the integrity of the coating.

An alternative approach was to embed thermocouples into one TEOS-coated RCC specimen. Specimen 9 was selected for this purpose and thereafter used exclusively for temperature control. In determining the temperature of the two test locations (A and B) as a function of the temperature at the control block (see

fig. 5), specimen 9 was mounted alternately in locations A and B. The control signal of the temperature profile was adjusted until the temperature histories at both A and B were as close as possible to the nominal Shuttle profile . Because of the effects of air pressure on the heat transfer to the specimens, the nominal mission air pressure profile was maintained during adjustments to the temperature profile. The final result of this iteration process is shown in figure 12. The rapid increase in temperature at the beginning and the end of the profile made it very difficult to heat and cool the specimen rapidly enough to match the profile. The test system followed the nominal profile quite well through the maximum temperature region but was unable to match the rapid cooling that occurred late in the profile.

Pressure Calibration

The objective of the pressure calibration was to control the chamber pressure to within 267 Pa of the nominal profile when the nominal pressure was below 13.3 kPa and to within 666 Pa of the nominal profile when the nominal pressure was above 13.3 ka.

For calibration of the pressure profile, the local pressure at the specimen location was assumed to be the same as that at the system pressure sensor. This assumption is reasonable since the pressure changes in the profile are not rapid and the pressure chamber has no significant baffles. The sensor is a capacitance type transducer whose inlet port is located on a

cold wall of the vacuum chamber approximately 200 mm from the center of the heated zone.

The results of the system air pressure calibration are shown in figure 13. During most of the mission profile, the chamber air pressure was within the desired tolerance. The short periods when the pressure is out of tolerance are a result of the closing and/or opening of the pressure control solenoid valves. These valves are necessary to limit the flow of the pressurized (approximately 21 kPa) inlet air to the servo-controlled needle valves which control chamber air pressure. Chamber pressure returns to nominal as soon as the servo valves can respond to the pressure surge caused by the solenoid valves. Air pressure errors were minimized by interactively adjusting the pressure command signal, the timing of the solenoid valve operation, and the amount of vacuum pumping on the vacuum chamber.

Load Calibration

The objective of the load calibration was to control the stress in the specimen to within 5 percent or $\pm$17 kPa, whichever is greater, of the nominal Shuttle profile.

The load trains for locations A and B were calibrated using a load cell which, in turn, had been calibrated using National Bureau of Standards traceable deadweights. Load profile calibration curves demonstrated that the load control consistently held the load on the specimens to within the

desired tolerance. Selected points are compared with the nominal profile in figure 14.

Calibration Missions

To assess the effect of temperature and pressure control on the adequacy of mission simulation, a series of simulated mission cycles was applied to the TEOS-coated RCC calibration specimen in both positions A and B. The objective was to match the calculated mass loss in each position with the nominal profile and the Vought Corporation mass loss equation in Appendix C (0.910 g/m^2 per mission). As previously noted, the temperature was not well matched during the rapid increase in temperature at the beginning of the mission or during the rapid cooling that occurred at the end of the mission. The slow cooling of the calibration specimen, when the pressure was high, caused the mass loss during simulation to be higher than nominal. Two changes were made in the simulation to bring the temperatures at all points of the specimen in line during the period when the maximum stresses were applied and to match the nominal mass loss per mission. First, a 1000 second hold was placed in the temperature profile after 400 seconds to allow temperatures in the specimen to equilibriate before maximum stresses were applied. In order to maintain correct simulation of all parameters during periods of peak temperatures, the pressure and stress profiles were held at initial values for 1000 seconds before being allowed to proceed. Thus after 1400 seconds had elapsed, all

parameters were again in sequence. Second, the simulated mass loss was brought into tolerance by rapidly evacuating the test chamber 1710 s into the mission. The rapid evacuation prevented any oxidation during the period when temperatures greatly exceeded nominal. Using the above procedures, the calculated mass loss at positions A and B was very closely matched with the calculated nominal mass loss (fig. 15). Figure 16 shows the calcualted mass loss using actual chamber temperature and pressures recorded during test series III compared with calculated mass loss using nominal values. The values from test series III were adjusted to account for the differences in temperatures at the various temperature stations in locations A and B as a function of the control temperatures that were obtained during calibration procedures. Even after 100 missions the calculated nominal and calculated actual values of mass loss are in good agreement.

APPENDIX C

Vought Corporation Mass-Loss Prediction Equation

Equation (C1) is the empirical mass loss prediction equation used during the experiments reported herein. This equation was derived by the Vought Corporation (unpublished data) for the purpose of Shuttle design.

$$\dot{m} = \dot{m}'_D P^{n'} \left\{ \frac{1 + Bm_L}{\left[1 + K'_1 \exp\left(E'_1 / RT\right)\right]\left[1 + K'_3 \exp\left(E'_3/RT\right)\right]} - \frac{1}{1 + K'_2 \exp\left(E'_2 / RT\right)} \right\} \qquad \text{(C1)}$$

where

$\dot{m}$ mass-loss rate, kg/m^2-s

m_L accumulated mass loss, kg/m^2, $\int_0^t \dot{m}\, dt$, where t is mission time in seconds

$\dot{m}'_D = 1.367 \times 10^{-5} \quad \frac{kg}{m^2\text{-s-atm}^n}$

$B = -7.324 + \frac{20\ 300\ K}{T}$

$K'_1 = 9.231 \times 10^{-6}$

$\frac{E'_1}{R} = 9811\ K$

$K'_2 = 6.135 \times 10^{-6}$

$\frac{E'_2}{R} = 15\ 183.33\ K$

$K'_3 = 2.84 \times 10^{-9}$

$\frac{E'_3}{R} = 12\ 177.78\ K$

$n' = 0.62$

P pressure, atm

n' = 0.62

P pressure, atm

T temperature, K

REFERENCES

1. Medford, J.E.: Multi-Cycle Plasma Arc Evaluation of Oxidation Inhibited Carbon-Carbon Material for Shuttle Leading Edges. ASME Paper Number 72-ENAV-26, August 1972.

2. McKinis, F. K.: Shuttle LESS Subsurface Attack Investigation. LTV Aerospace Corporation Report No. 221Rp00241, Vought Corporation, December 1974.

3. Medford, J.E.: Prediction of Oxidation Performance of Reinforced Carbon-Carbon Material for Space Shuttle Leading Edges. AIAA Paper 75-730, 10th Thermophysics Conference, 1975.

4. Dicus, Dennis L.; Hopko, Russell, N.; and Brown, Ronald D.: Ablative Performace of Uncoated Silicone Modified and Shuttle Baseline Reinforced Carbon Composites. NASA TN D-8358, December 1976.

5. Curry, Donald M.; Johansen, K. J.; and Stephens, Emily W.: Reinforced Carbon-Carbon Oxidation Behavior in Convective and Radiative Environments. NASA TP-1248, August 1978.

6. Stroud, C. W. and Rummler, Donald R.: Mass Loss of a TEOS Coated, Reinforced Carbon-Carbon Composite Subjected to a Simulated Shuttle Entry Environment. NASA TM 81799, 1980.

7. Comm. on Metric Pract.: ASTM Practice Guide. NBS Handbook 102, U.S. Dept. Comm., March 10, 1967.

8. Miller, Irwin; and Freund, John E.: Probability and Statistics for Engineers. Prentice Hall, Inc., 1965.

TABLE I.- DIMENSIONS OF TEOS-COATED RCC SPECIMENS

Specimen	Thickness				
	t_1, mm	t_2, mm	t_3, mm	t_4, mm	t_5, mm
1	5.740	5.784	5.809	5.809	5.839
2	5.776	5.771	5.791	5.794	5.791
3	5.773	5.799	5.806	5.812	5.824
4	5.735	5.781	5.784	5.799	5.809
5	5.743	5.796	5.799	5.812	5.822
6	5.720	5.766	5.756	5.771	5.773
7	5.743	5.776	5.773	5.789	5.852
8	5.745	5.771	5.776	5.773	5.801

Specimen	Width							
	ℓ mm	w_1, mm	w_2, mm	w_3, mm	w_4, mm	w_5, mm	w_6, mm	w_7, mm
1	221.94	43.353	43.365	17.861	17.856	17.851	43.383	43.414
2	221.92	43.320	43.355	17.945	17.963	17.953	43.363	43.411
3	222.02	43.337	43.363	17.836	17.833	17.838	43.378	43.429
4	221.90	43.368	43.373	17.861	17.849	17.818	43.363	43.365
5	221.96	43.332	43.371	17.892	17.861	17.851	43.419	43.470
6	221.96	43.340	43.350	17.775	17.765	17.760	43.343	43.429
7	222.00	43.340	43.383	17.882	17.861	17.851	43.416	43.470
8	222.00	43.312	43.327	17.861	17.856	17.841	43.327	43.312

TABLE II. PHYSICAL CHARACTERISTICS OF TEOS-COATED RCC SPECIMENS

Specimen	Weighted Thickness t_w, mm	Effective Cross Section Area, mm^2	Calculated Surface Area, m^2	Bulk Density, g/cm^3
1	5.801	91.806	.01642	1.677
2	5.786	92.129	.01643	1.687
3	5.806	91.742	.01643	1.693
4	5.789	91.484	.01640	1.708
5	5.801	91.871	.01643	1.695
6	5.766	90.709	.01638	1.712
7	5.779	91.484	.01643	1.704
8	5.773	91.355	.01640	1.708
	Mass, Before Drying, g	Mass After Drying, g	Bulk Volume, cm^3	
1	64.365	64.107	38.485	
2	64.740	64.482	38.459	
3	65.141	64.813	38.532	
4	65.527	65.128	38.366	
5	65.174	64.858	38.503	
6	65.355	64.969	38.176	
7	65.467	65.169	38.474	
8	65.357	65.049	38.327	

TABLE III.- NOMINAL MISSION PROFILE OF LUG ATTACHMENT AREA

TIME, S	TEMPERATURE, K	PRESSURE, ATM
0	328	$<10^{-6}$
100	565	2.0×10^{-5}
200	758	1.1×10^{-4}
300	1031	8.0×10^{-4}
400	1338	4.7×10^{-3}
500	1555	.012
600	1597	.015
700	1611	.018
800	1614	.021
900	1625	.026
1000	1634	.035
1100	1612	.056
1200	1546	.061
1300	1399	.057
1400	1263	.057
1500	1139	.066
1600	991	.071
1700	853	.103
1800	728	.122
1900	550	.123
2000	372	.180
2100	328	.402
2200	328	.855
2260	328	1.000

TIME, S	STRESS, MPa
0	0
400	8.274
1000	8.274
2000	4.551
2200	8.274
2210	0

TABLE IV.- SUMMARY OF CUMULATIVE MASS-LOSS DATA

Number of Missions	Test Series I	
	Specimen 1 Location A No Load	Specimen 2 Location B Load
	Mass Loss	Mass Loss
	g/m^2	g/m^2
1	5.419	7.958
5	8.299	7.567
10	9.813	9.227
15	12.059	11.522
20	14.304	13.865
25	16.599	16.306
30	19.430	19.040
35	21.920	21.725
40	25.045	24.801
45	27.193	26.997
50	30.268	30.220

TABLE IV.- Continued.

Number of Missions	Test Series II	
	Specimen 3 Location A Load	Specimen 5 Location B No Load
	Mass Loss	Mass Loss
	g/m^2	g/m^2
5	9.042	8.348
10	10.545	9.764
15	12.986	11.863
20	15.525	14.207
25	18.015	16.257
30	20.651	18.747
35	23.482	21.041
40	26.314	23.727
45	28.609	26.216
50	31.635	28.853
55	34.955	31.635
60	38.275	34.467
65	42.083	37.543
70	45.549	40.472
75	49.308	43.596
80	53.311	46.623
85	57.412	49.796
90	61.464	52.823
95	65.419	55.557
100	92.156	59.219

TABLE IV.- Continued.

Number of Missions	Test Series III	
	Specimen 8 Location A No Load	Specimen 7 Location B Load
	Mass Loss	Mass Loss
	g/m^2	g/m^2
5	9.618	9.813
10	10.985	11.277
15	12.693	13.084
20	14.939	15.378
25	17.185	18.015
30	19.577	20.407
35	22.067	22.994
40	24.654	25.582
45	27.339	28.560
50	30.024	31.245
55	32.954	34.272
60	35.248	36.713
65	37.933	39.495
70	40.325	42.180
75	43.010	45.110
80	45.500	47.844
85	48.185	50.480
90	50.870	53.458
95	53.653	56.387
100	56.485	59.463

TABLE IV.- Concluded

Number of Missions	Test Series IV	
	Specimen 4 Location A Load	Specimen 6 Location B No Load
	Mass Loss	Mass Loss
	g/m^2	g/m^2
4	8.885	9.910
10	10.789	11.522
15	13.181	13.474
20	15.720	15.671
25	18.454	17.966
30	21.188	20.260
35	24.068	22.652
40	27.144	25.338
45	30.122	27.730
50	33.344	30.268

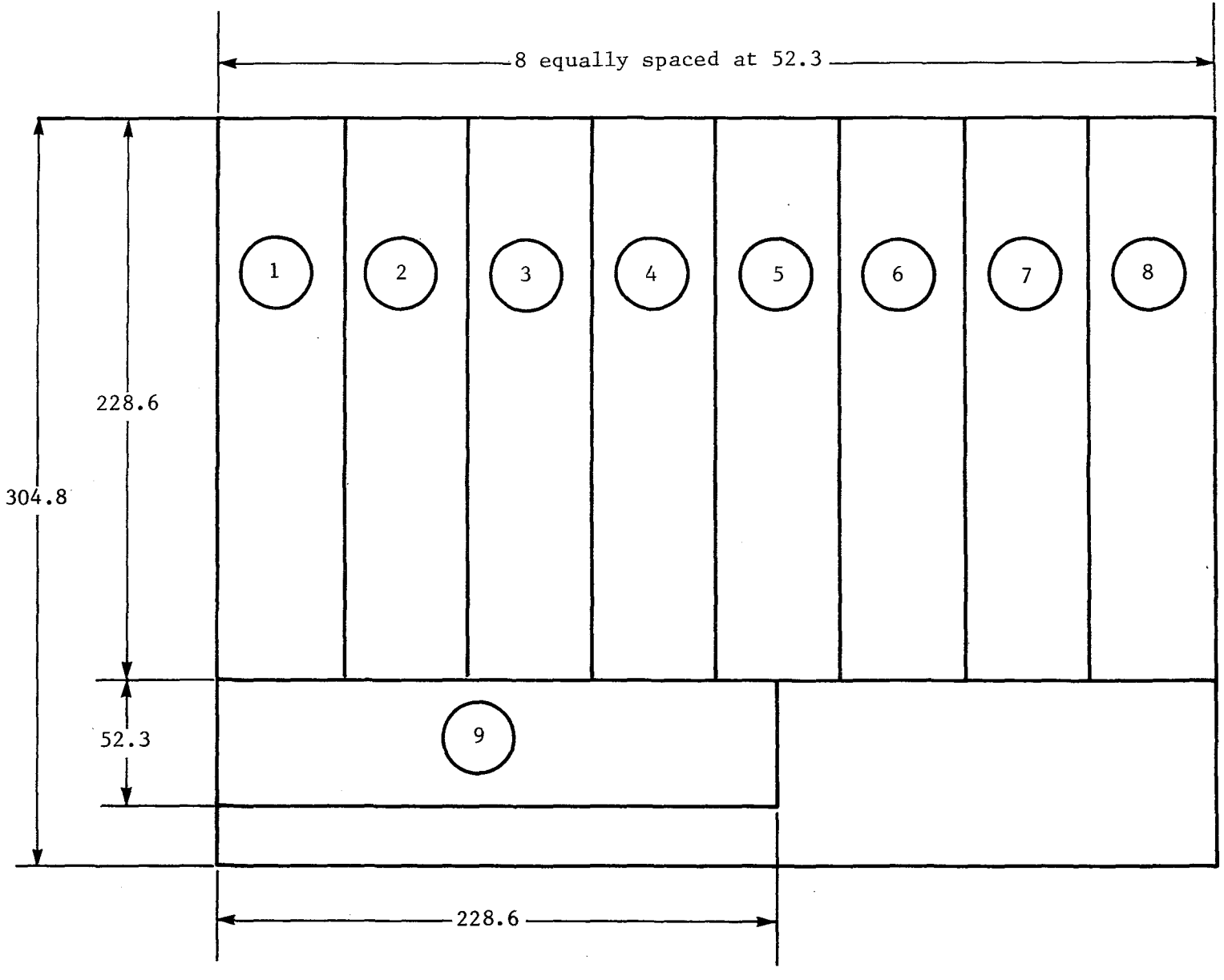

Figure 1.- Specimen layout for 19-ply reinforced carbon-carbon material blanks (Dimensions are in millimeters.)

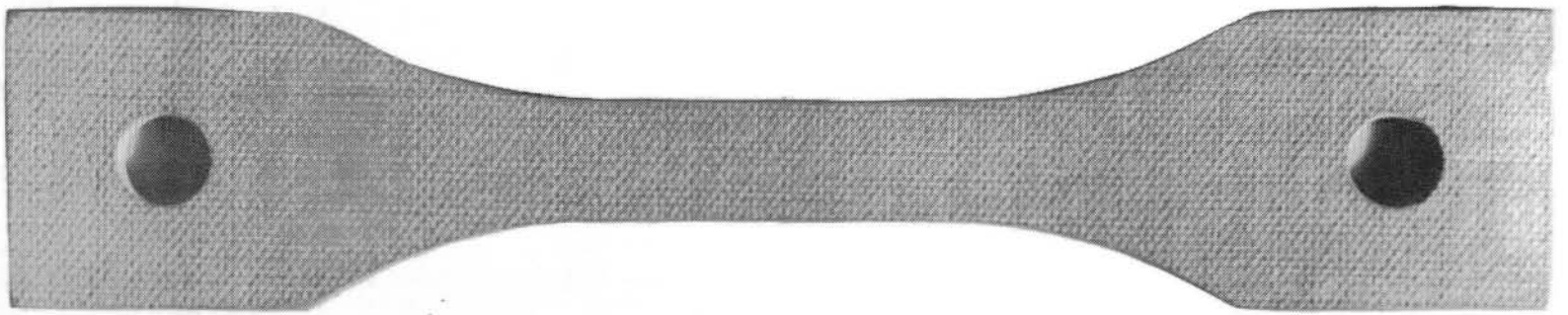

L-79-3291.1

Front

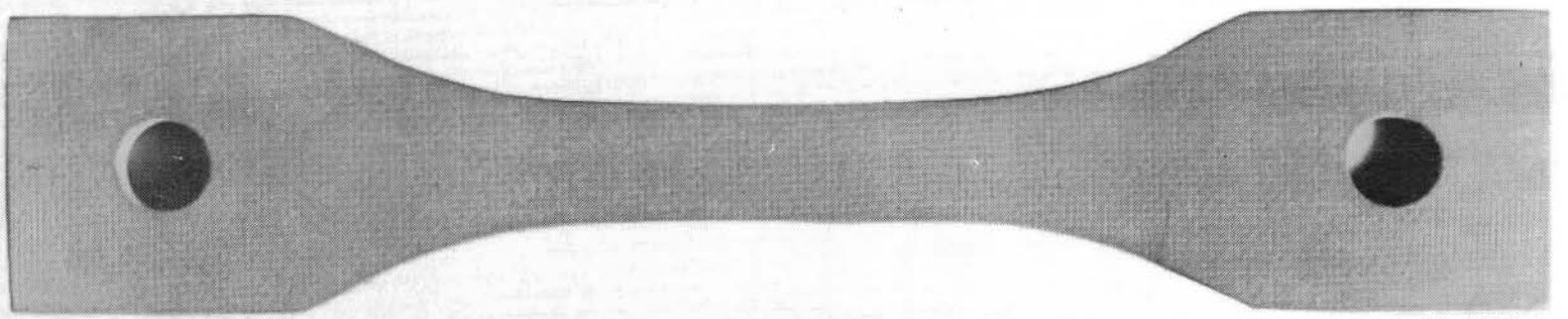

L-79-3292.1

Back

Figure 2.- As-received TEOS-coated RCC specimen 7.

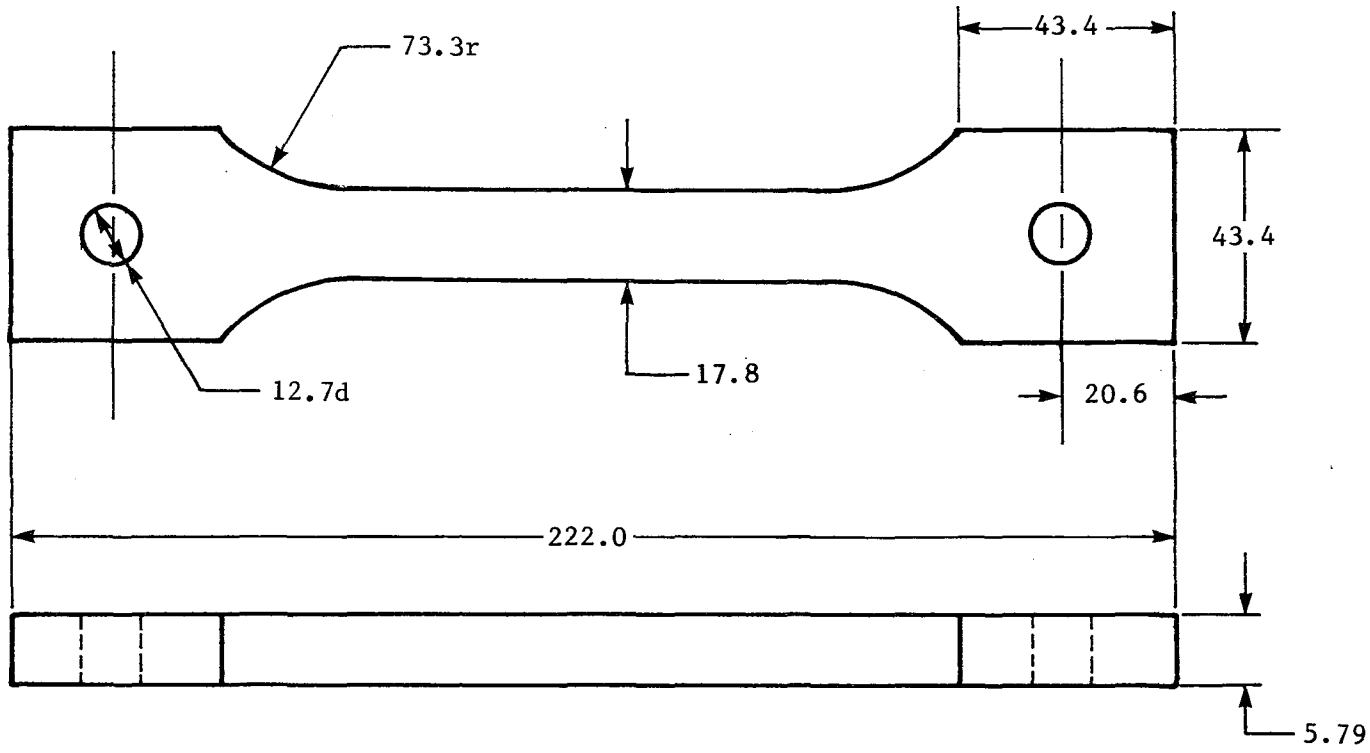

Figure 3.- Nominal dimensions of 19-ply TEOS-coated RCC specimens. (Dimensions are in millimeters.)

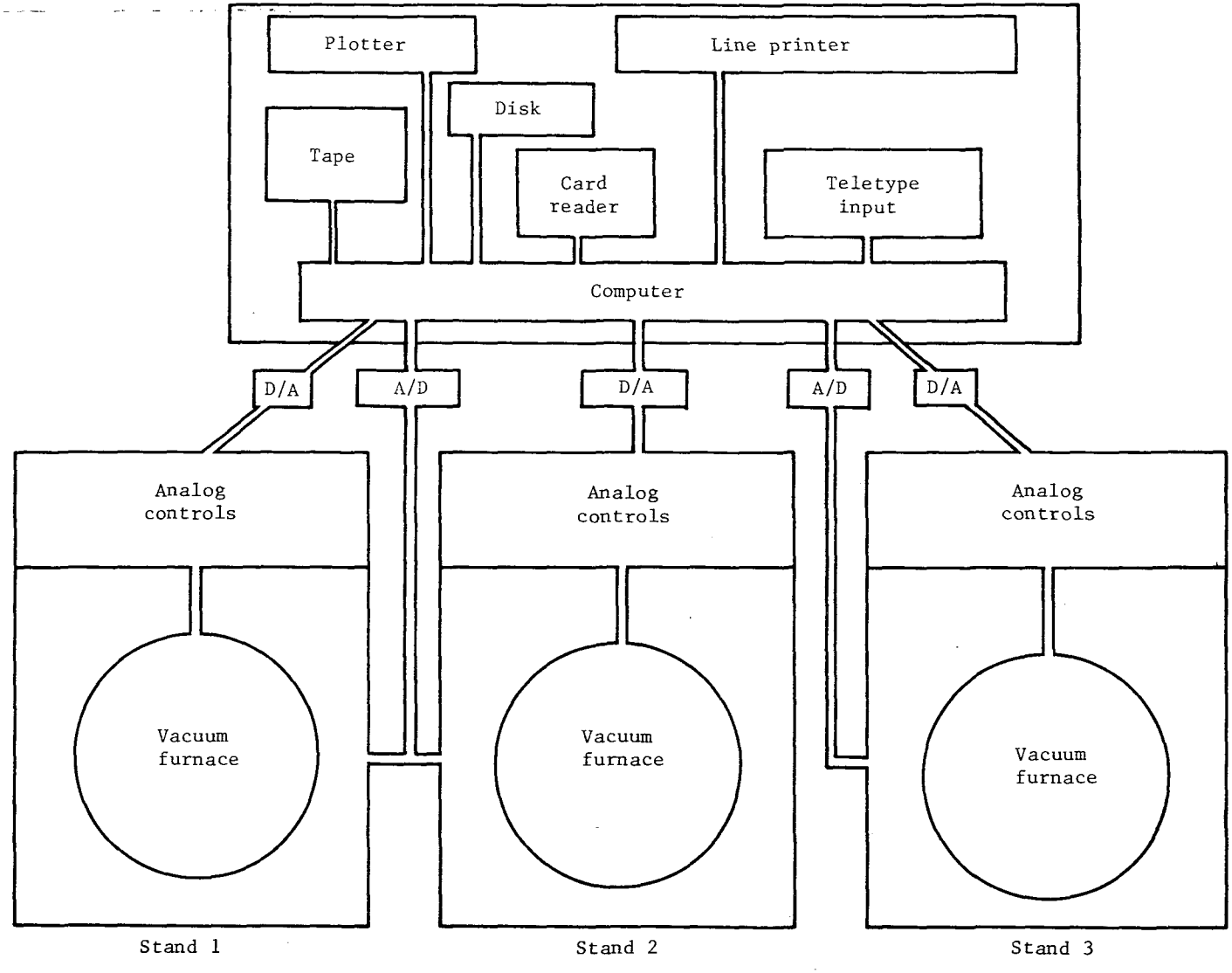

(a) Block diagram.

Figure 4.- Multiparameter test system.

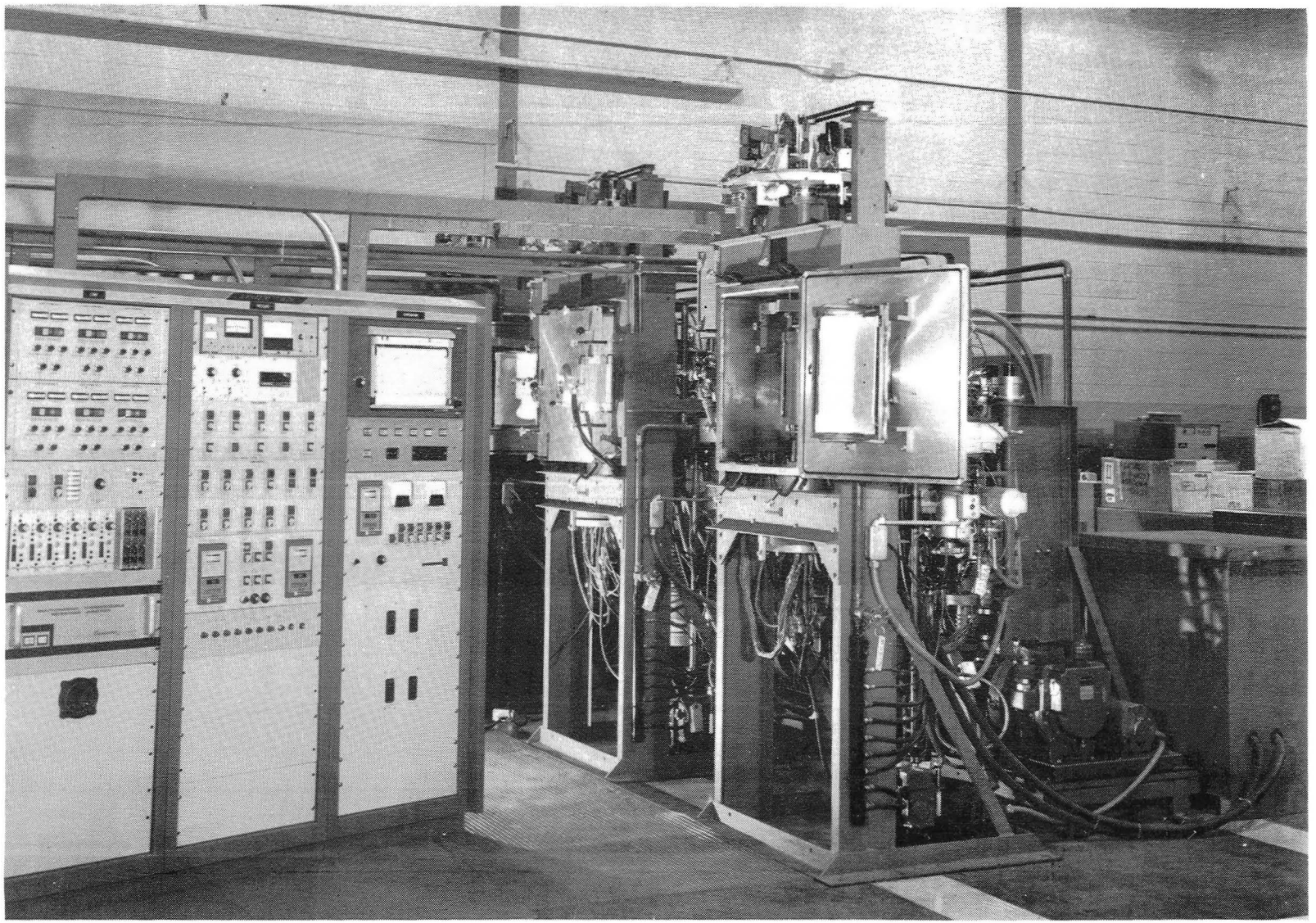

L-80-130

(b) Vacuum furnaces and analog controls.

Figure 4.- Concluded.

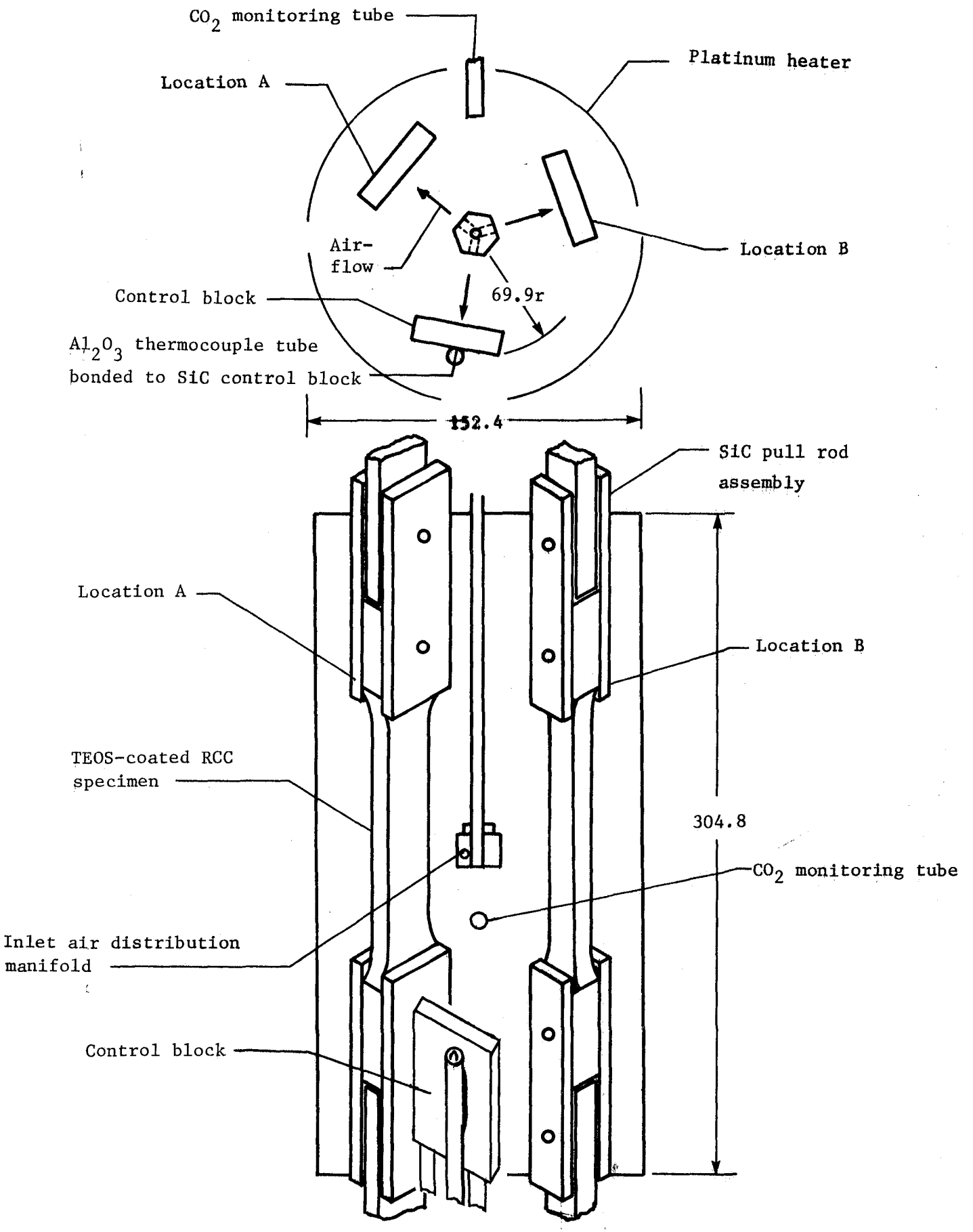

Figure 5.- Furnace and specimen configuration (mm).

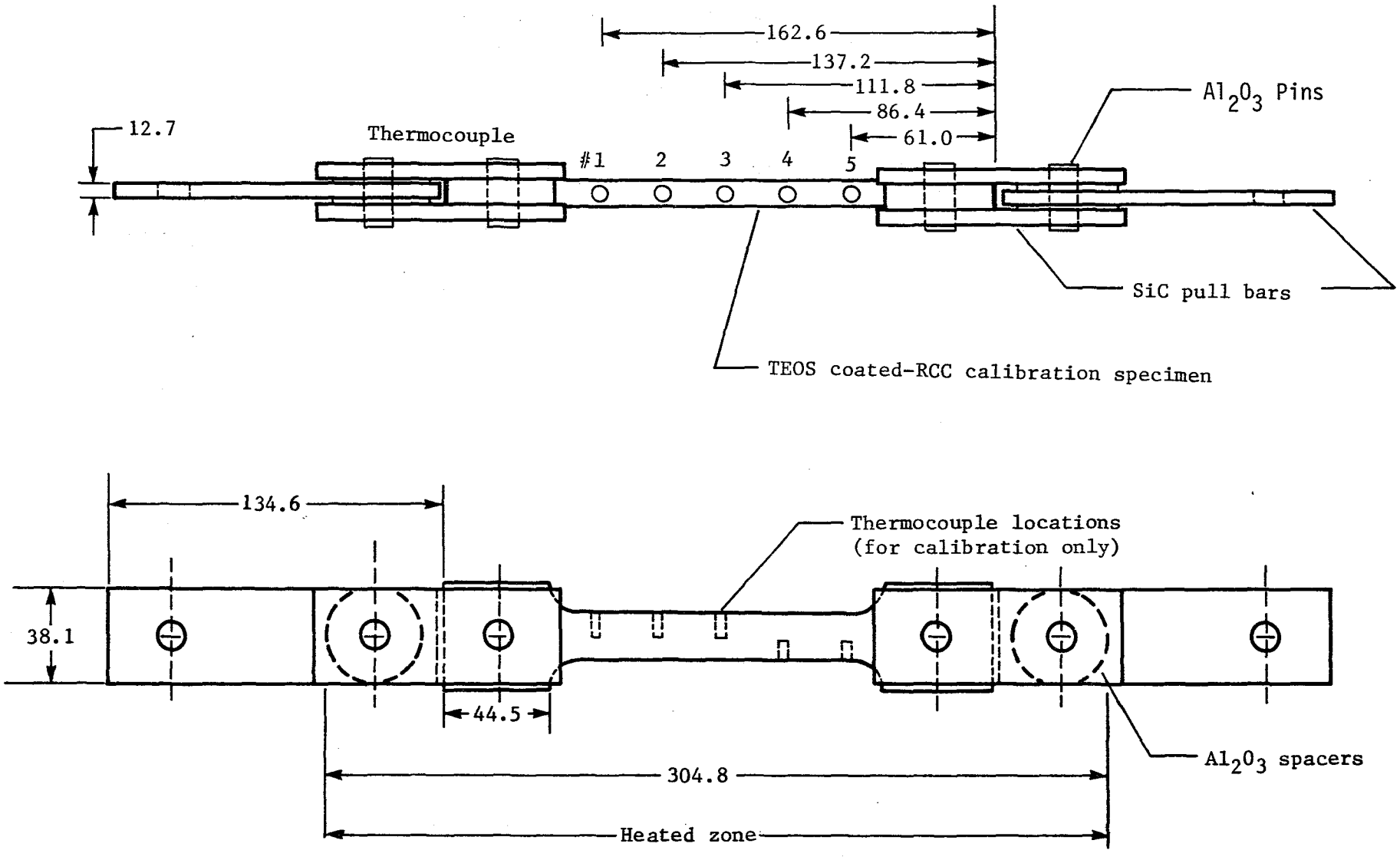

Figure 6.- Load train configuration with calibration specimen in place (mm).

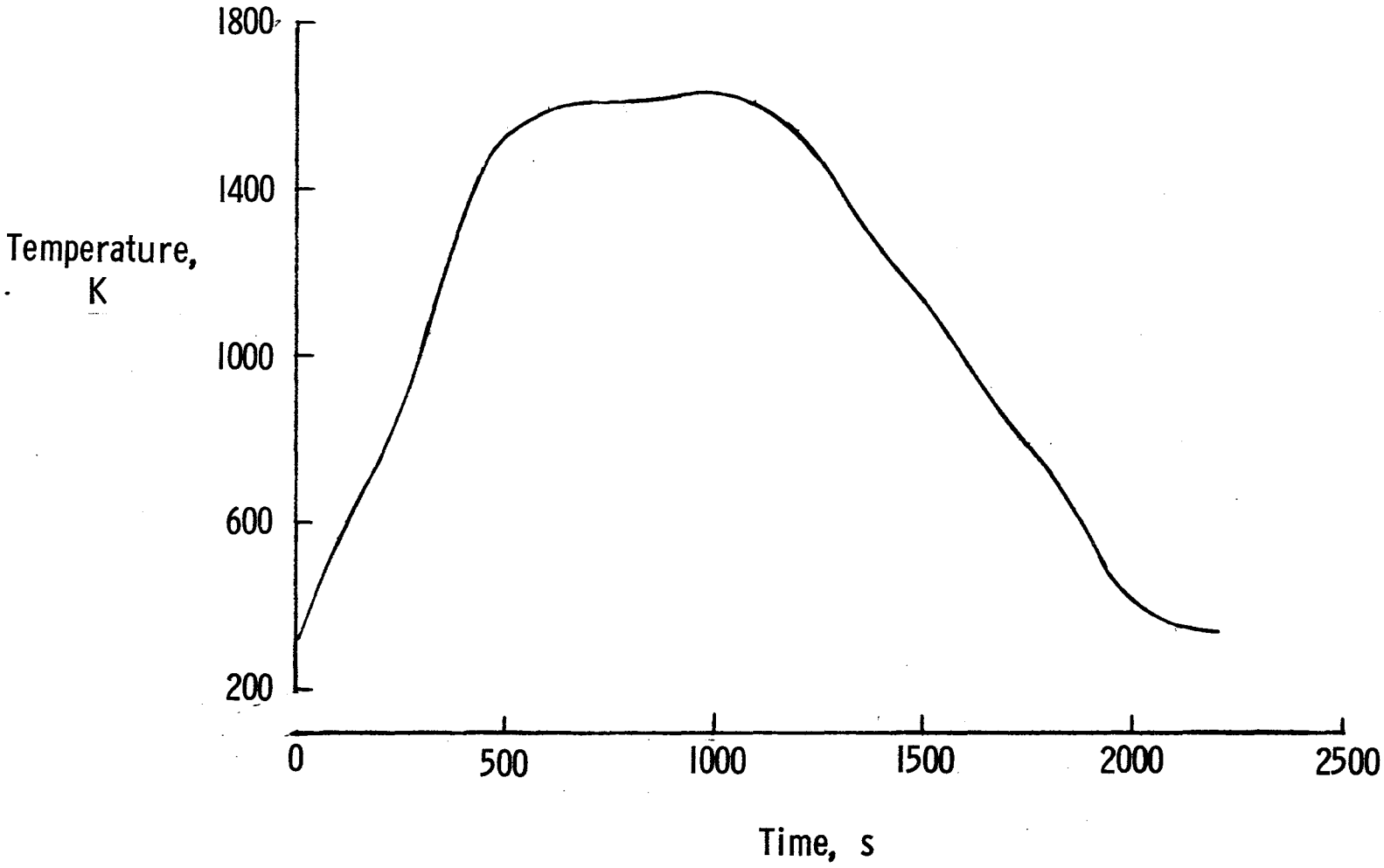

Figure 7.- Stagnation area mission histories.
(a) Temperature history.

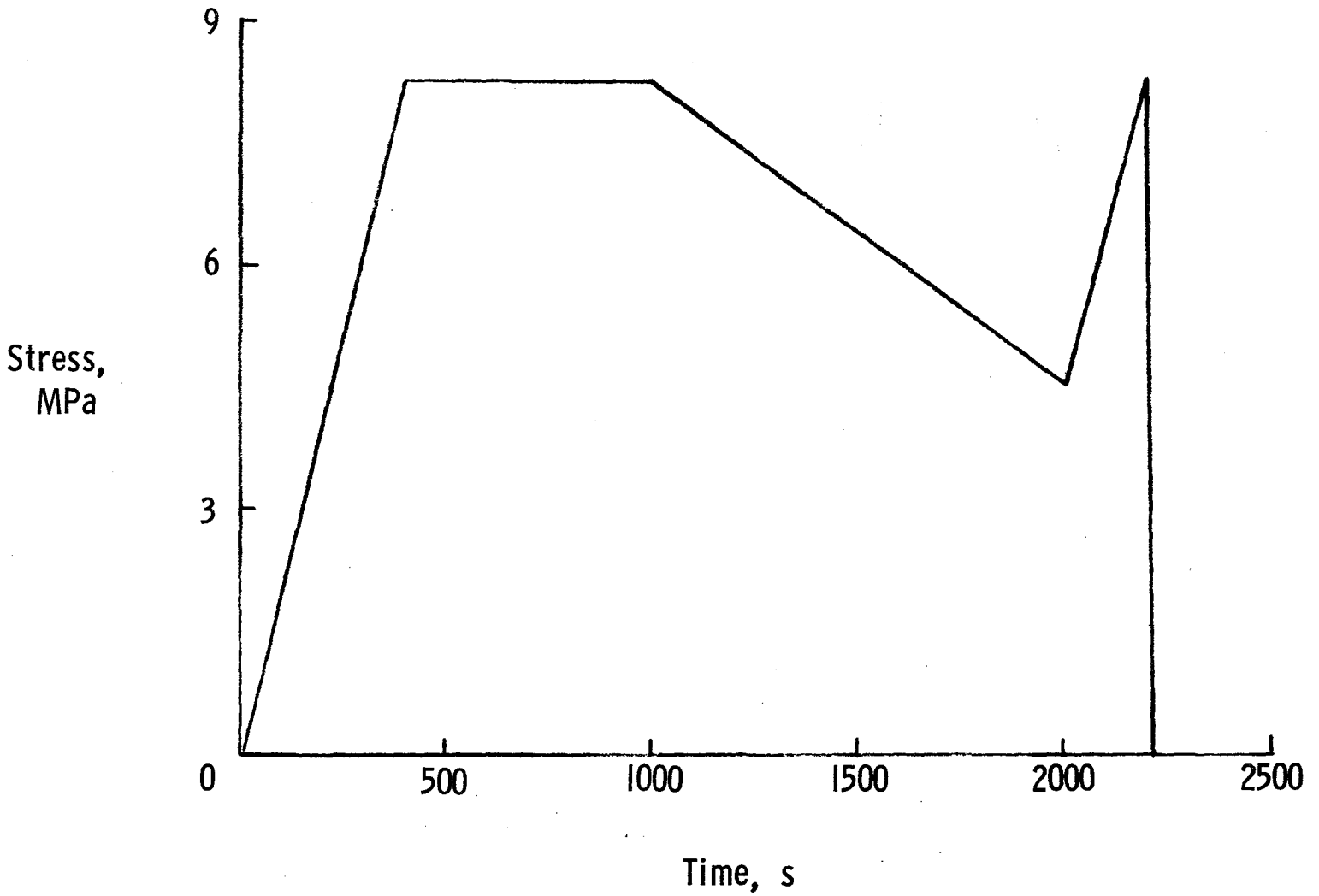

(b) Load history.

Figure 7.- Continued.

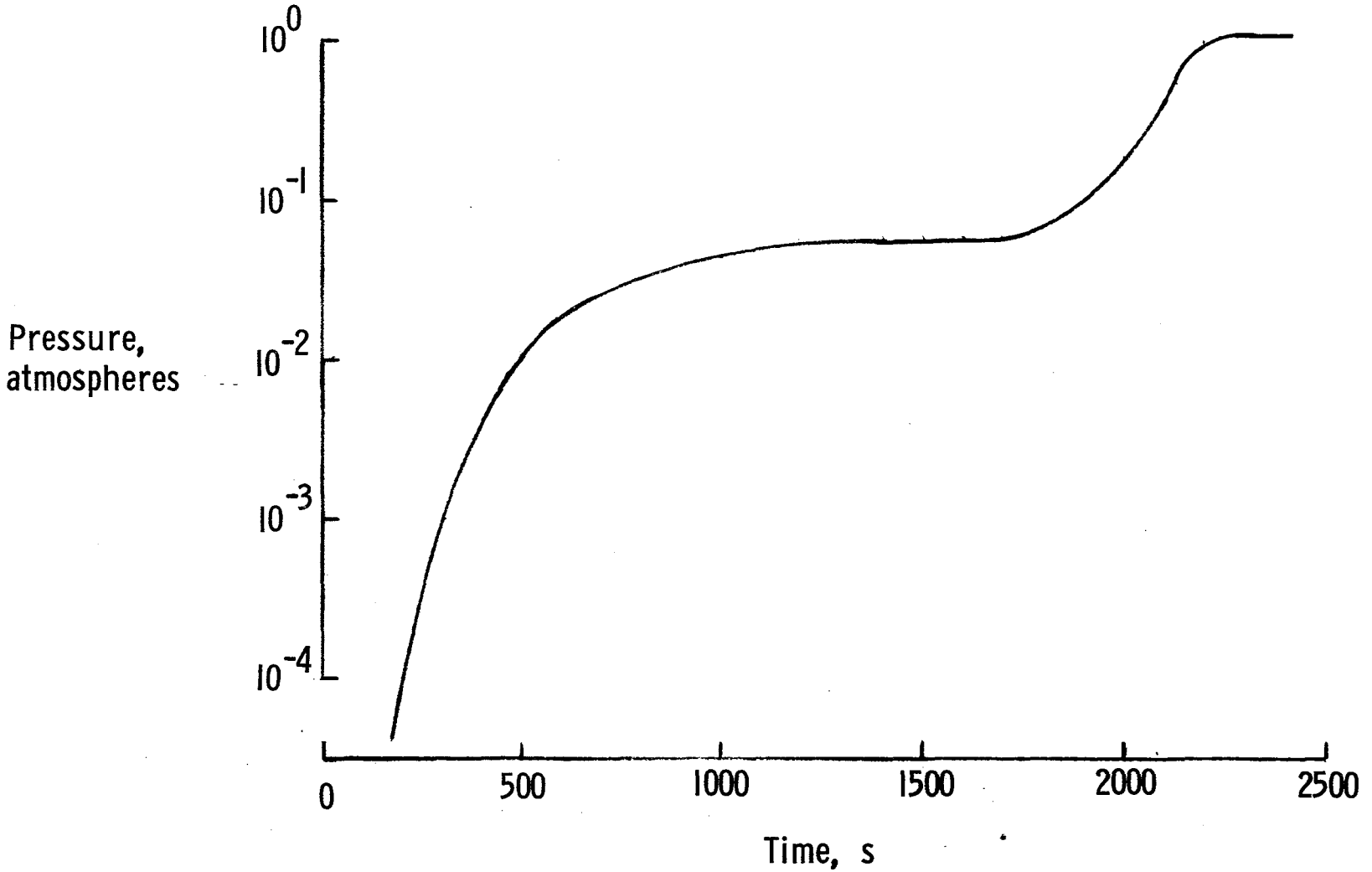

(c) Pressure history.

Figure 7.- Concluded.

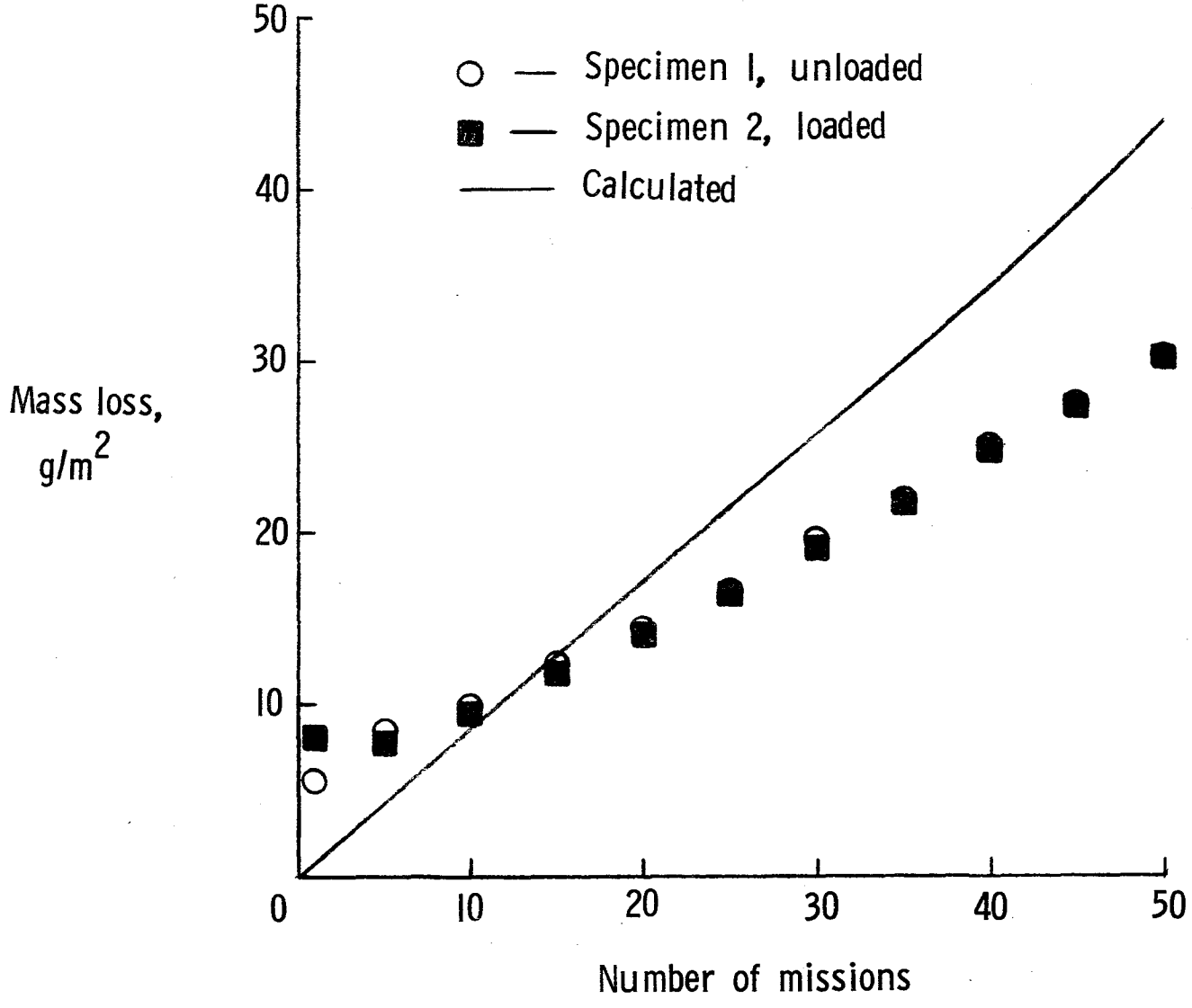

Figure 8.- Mass loss as a function of mission cycles.
(a) Test series I

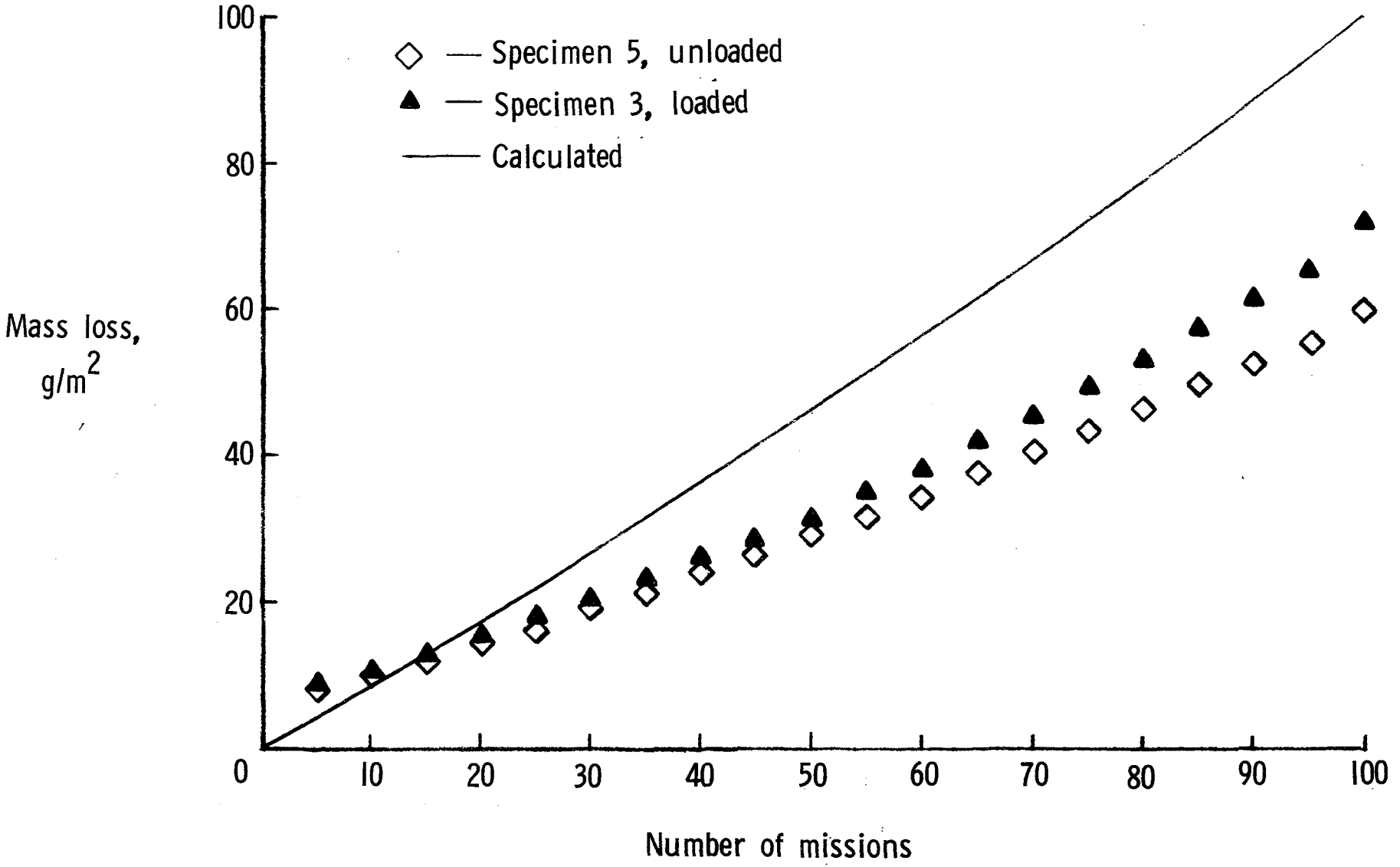

Figure 8.- Continued
(b) Test Series II

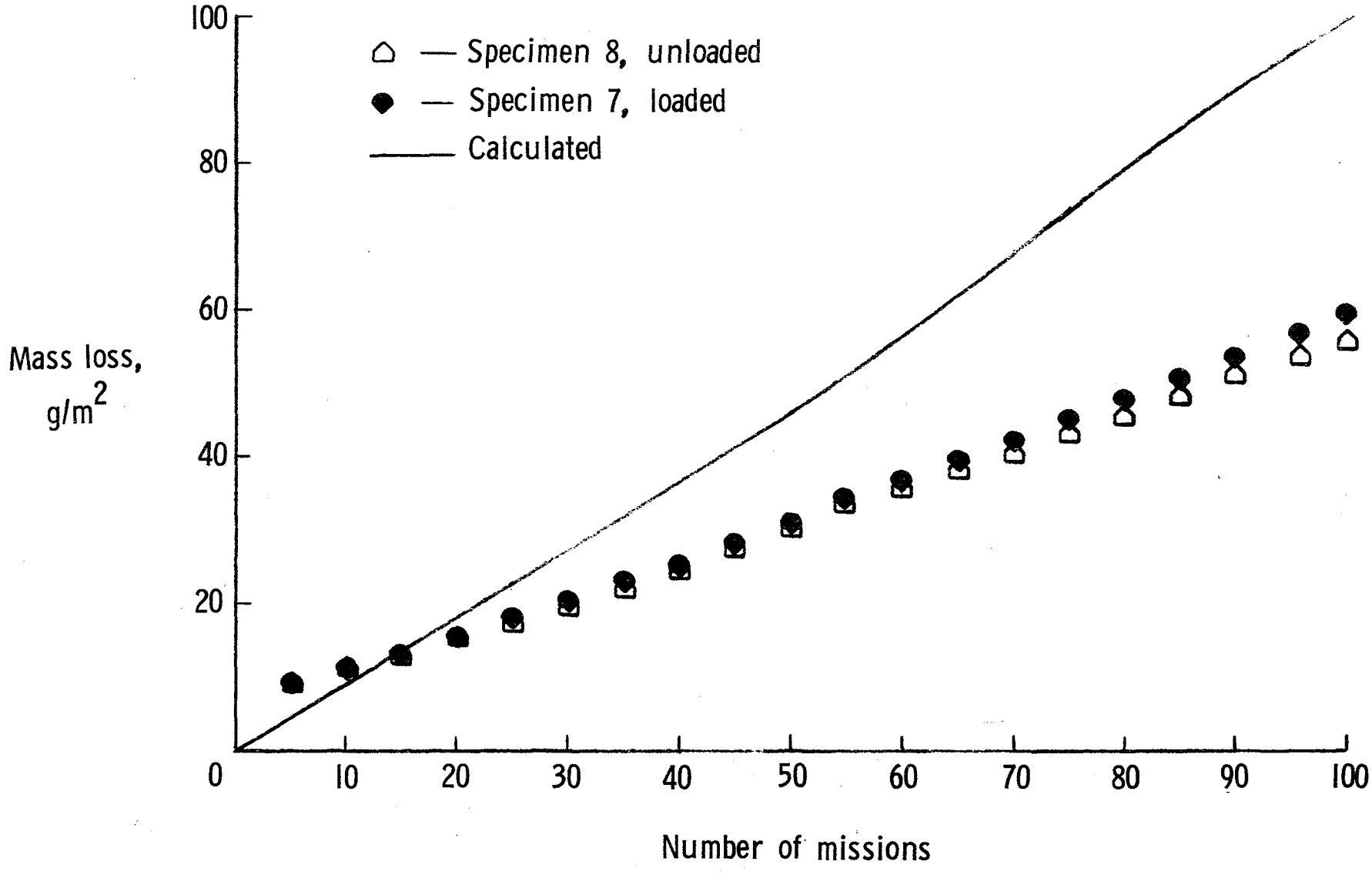

Figure 8.- Continued
(c) Test series III

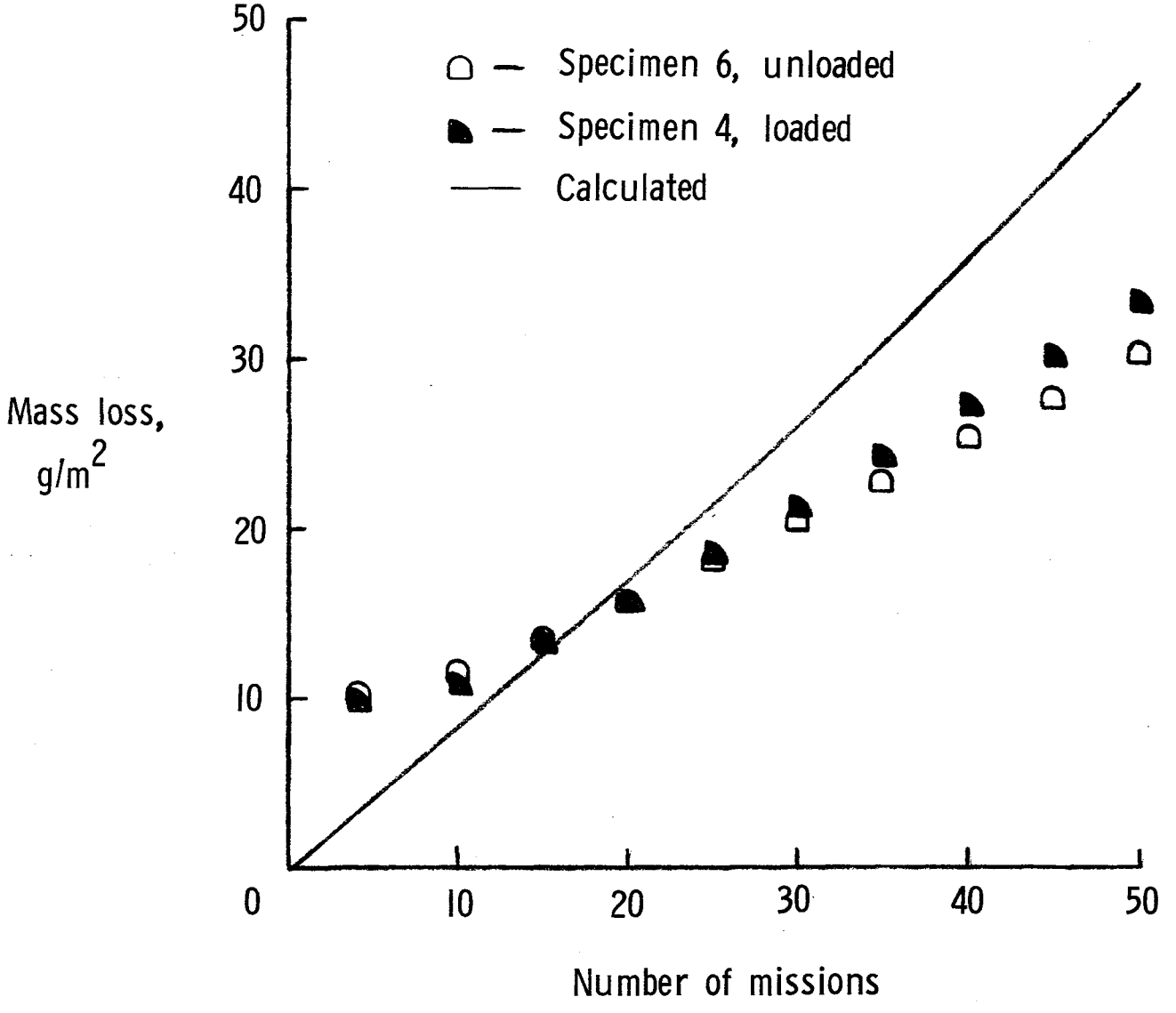

Figure 8.- Concluded
(d) Test series IV

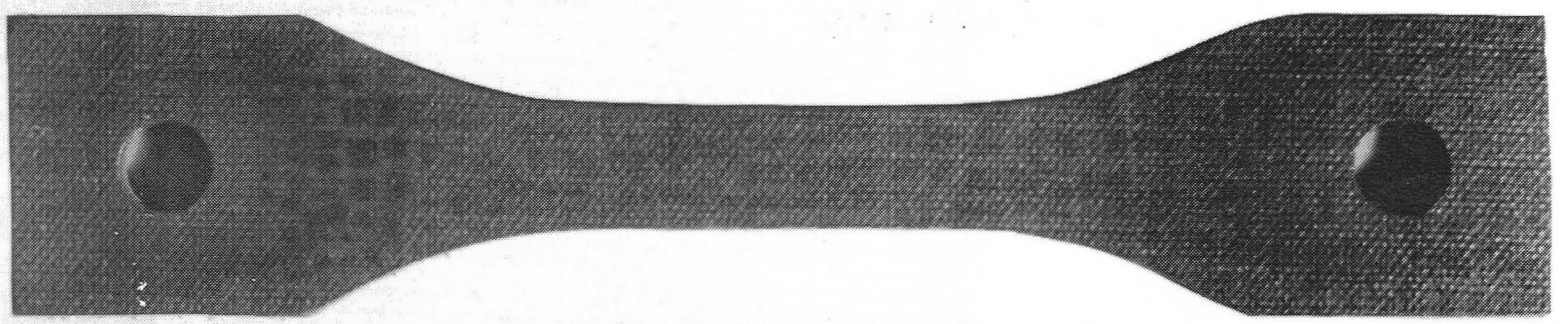

Front

L-79-3719.1

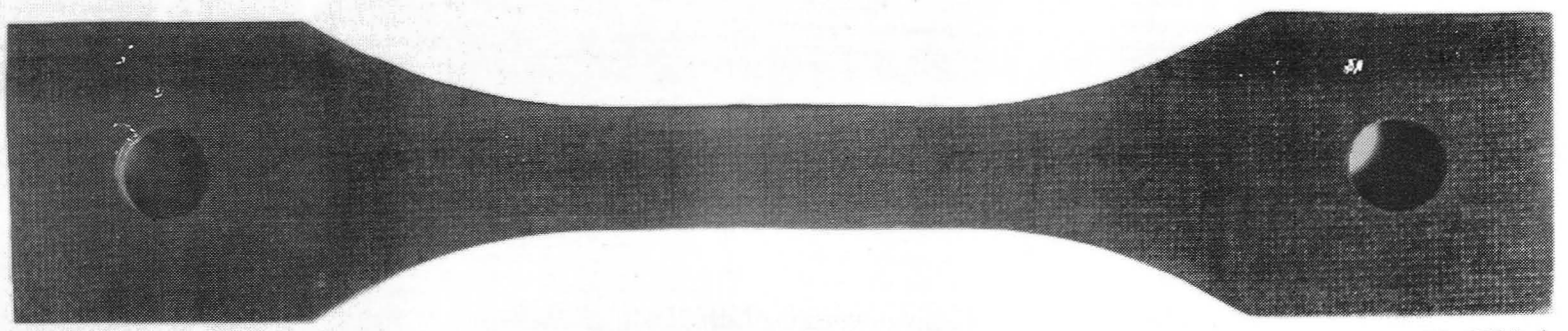

Back

L-79-3720.1

Figure 9.- Specimen 7 after 100 missions.

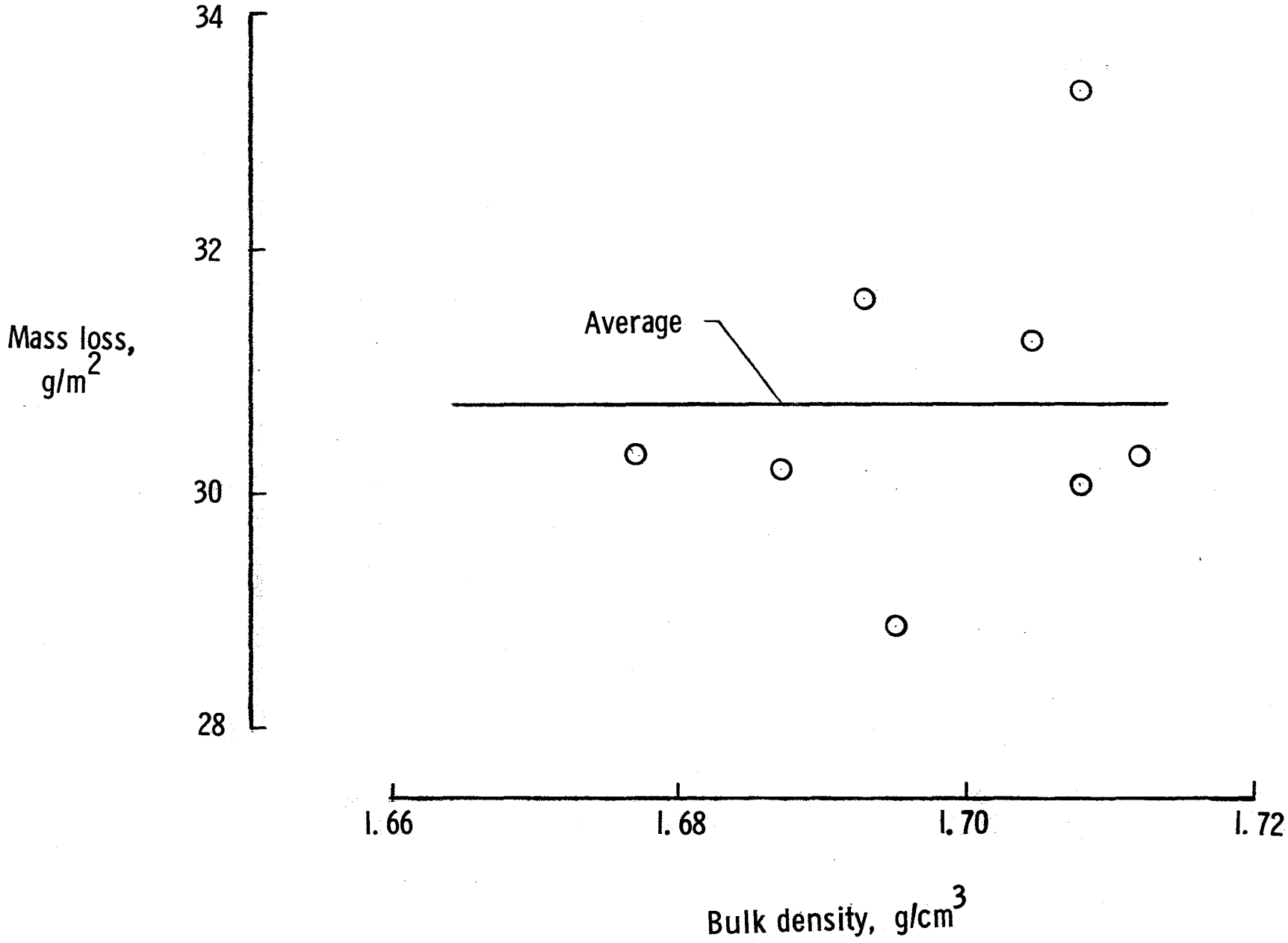

Figure 10.- Mass loss after 50 missions versus initial specimen density

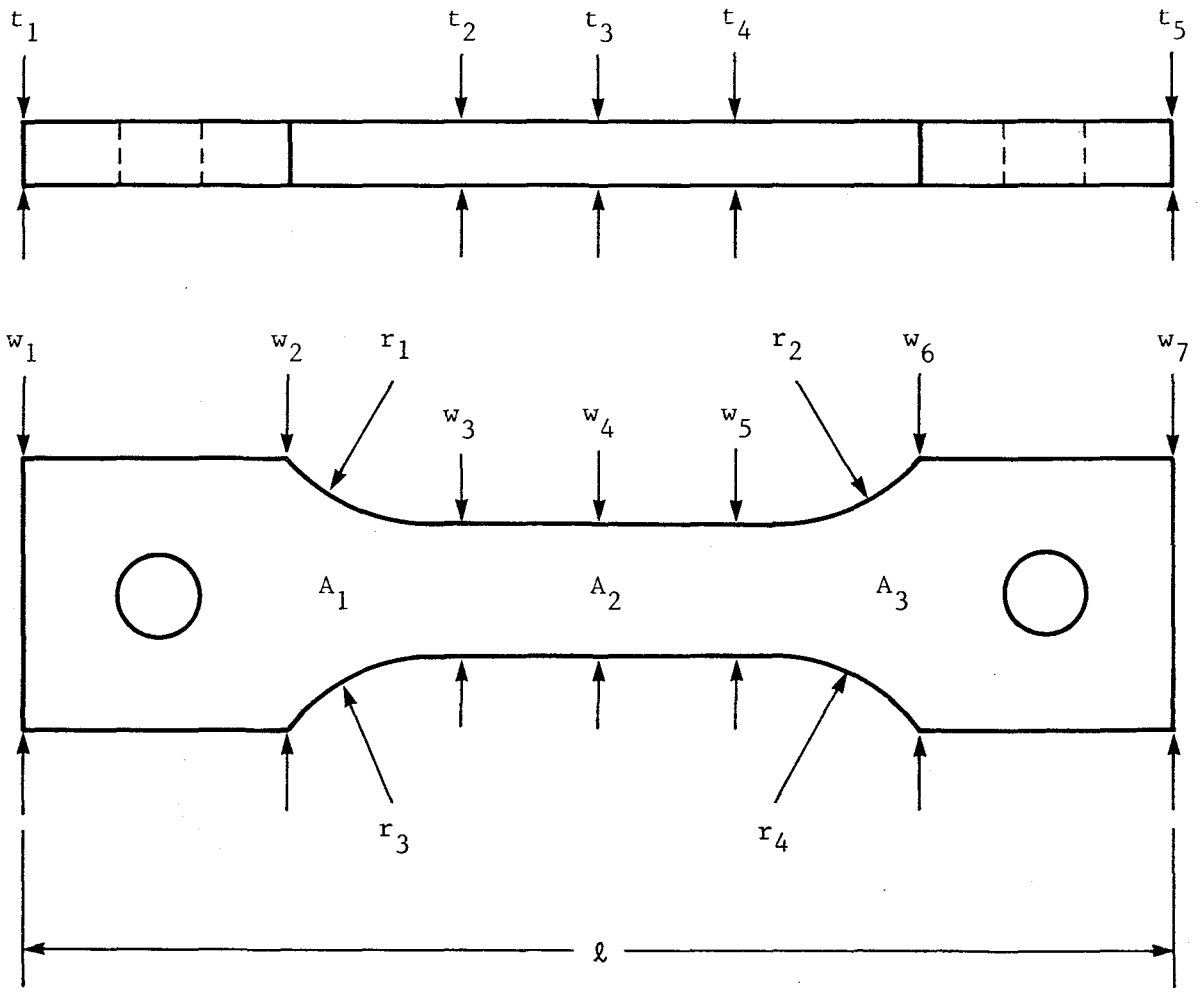

Figure 11.- Measurement locations on TEOS-coated RCC specimens.

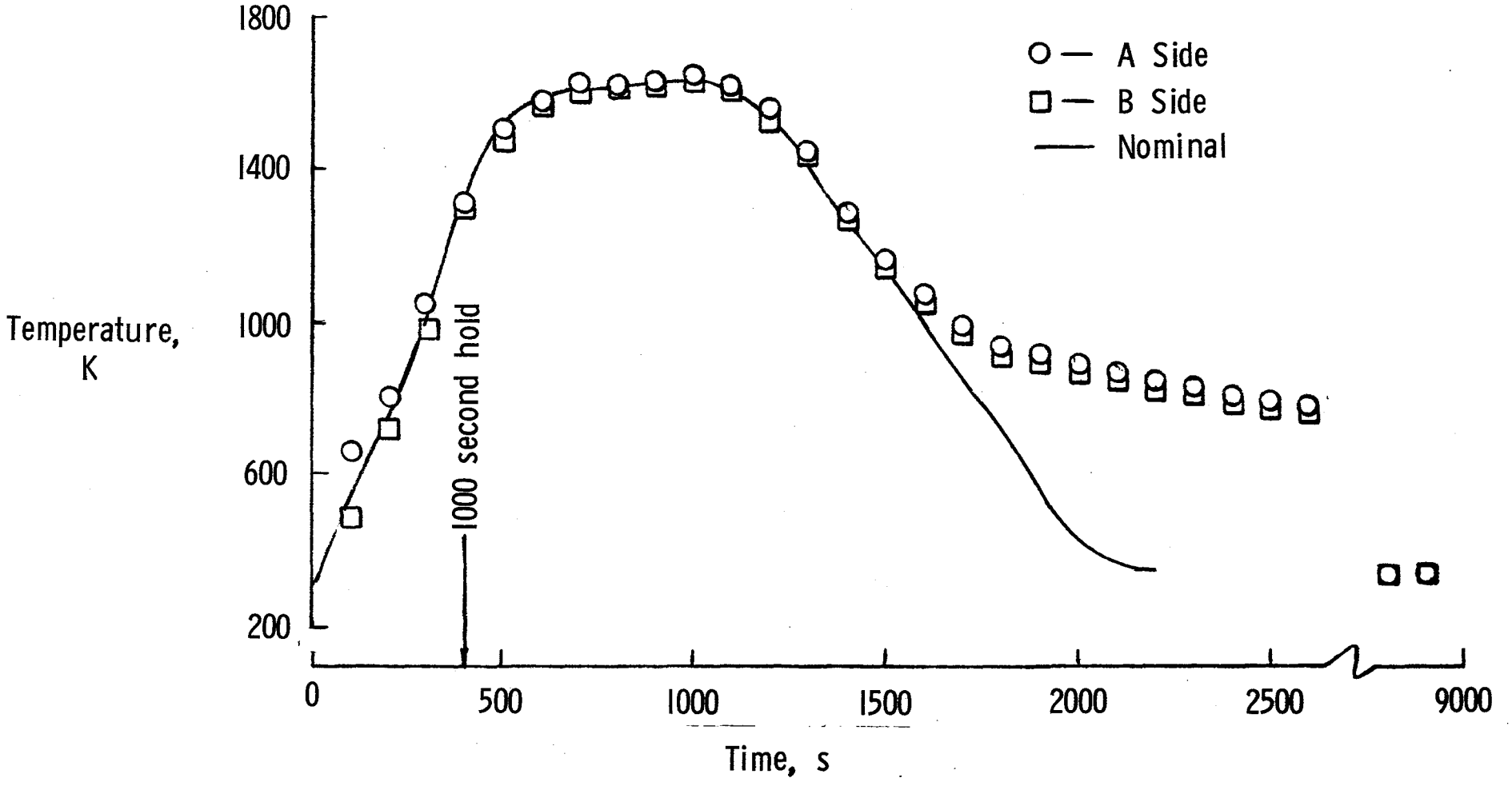

Figure 12.- Temperature profiles from calibration missions.

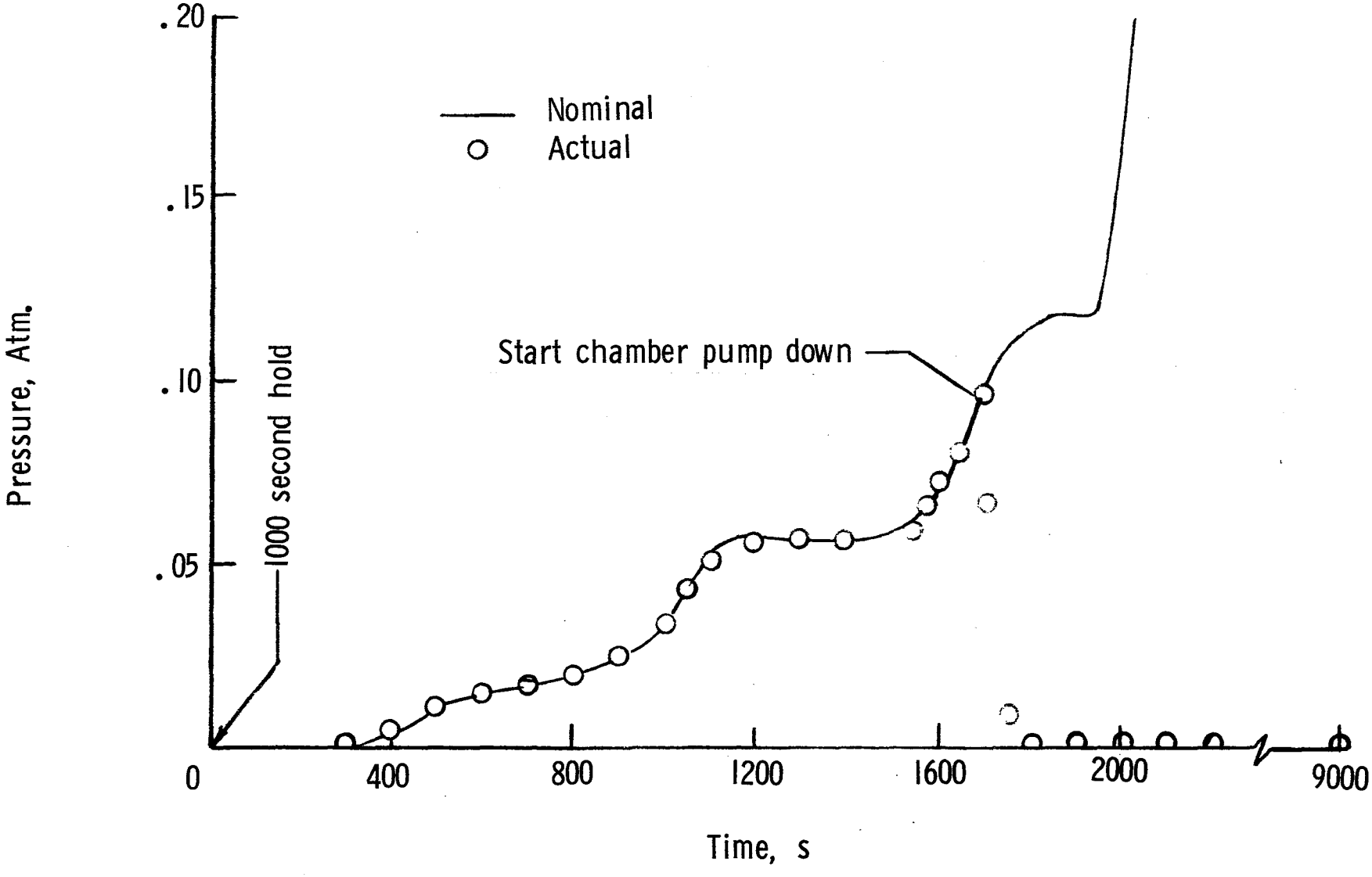

Figure 13.- Comparison of nominal and actual pressure profile for a typical calibration mission

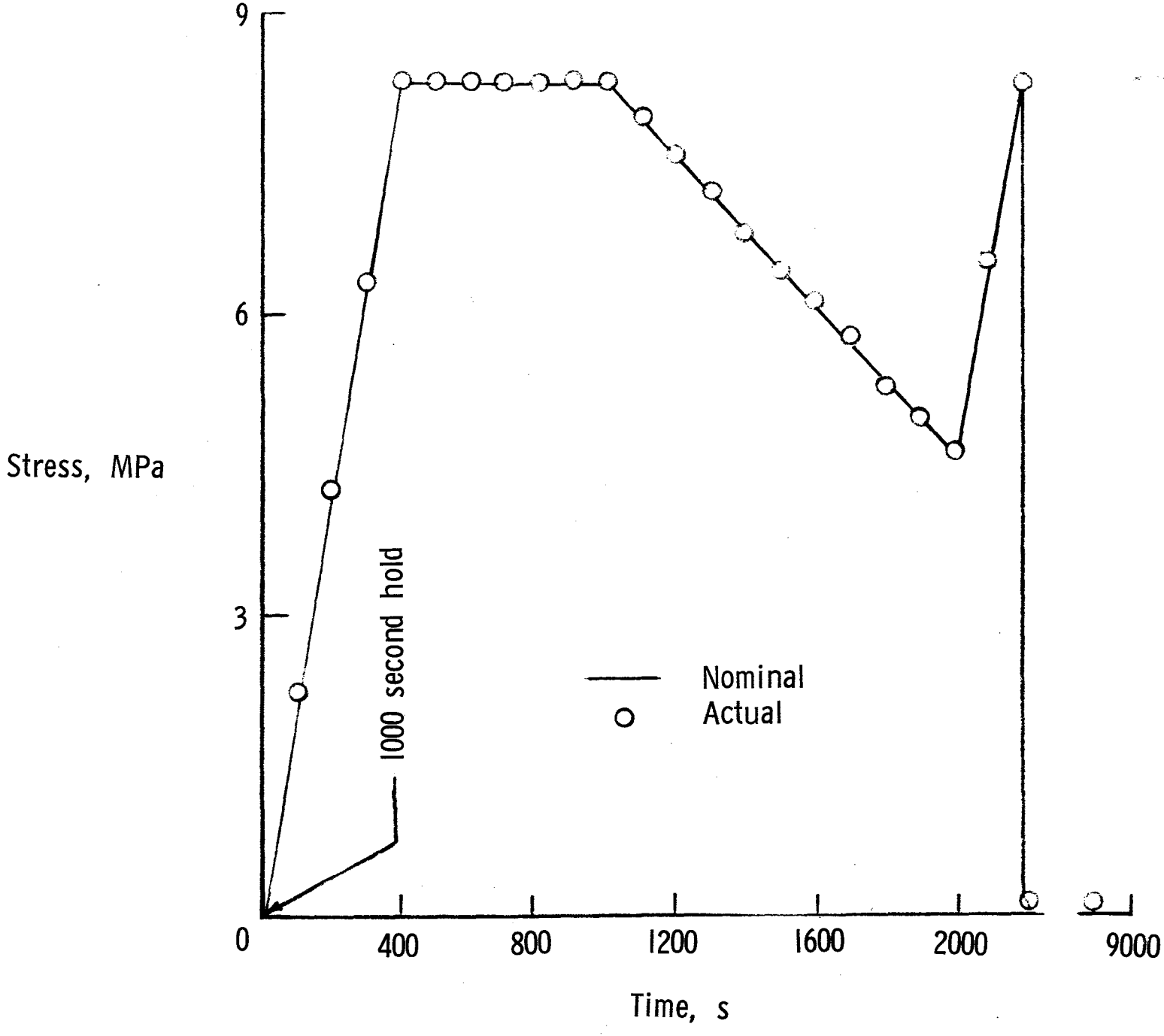

Figure 14.- Comparison of nominal and actual stress profile for a typical calibration mission

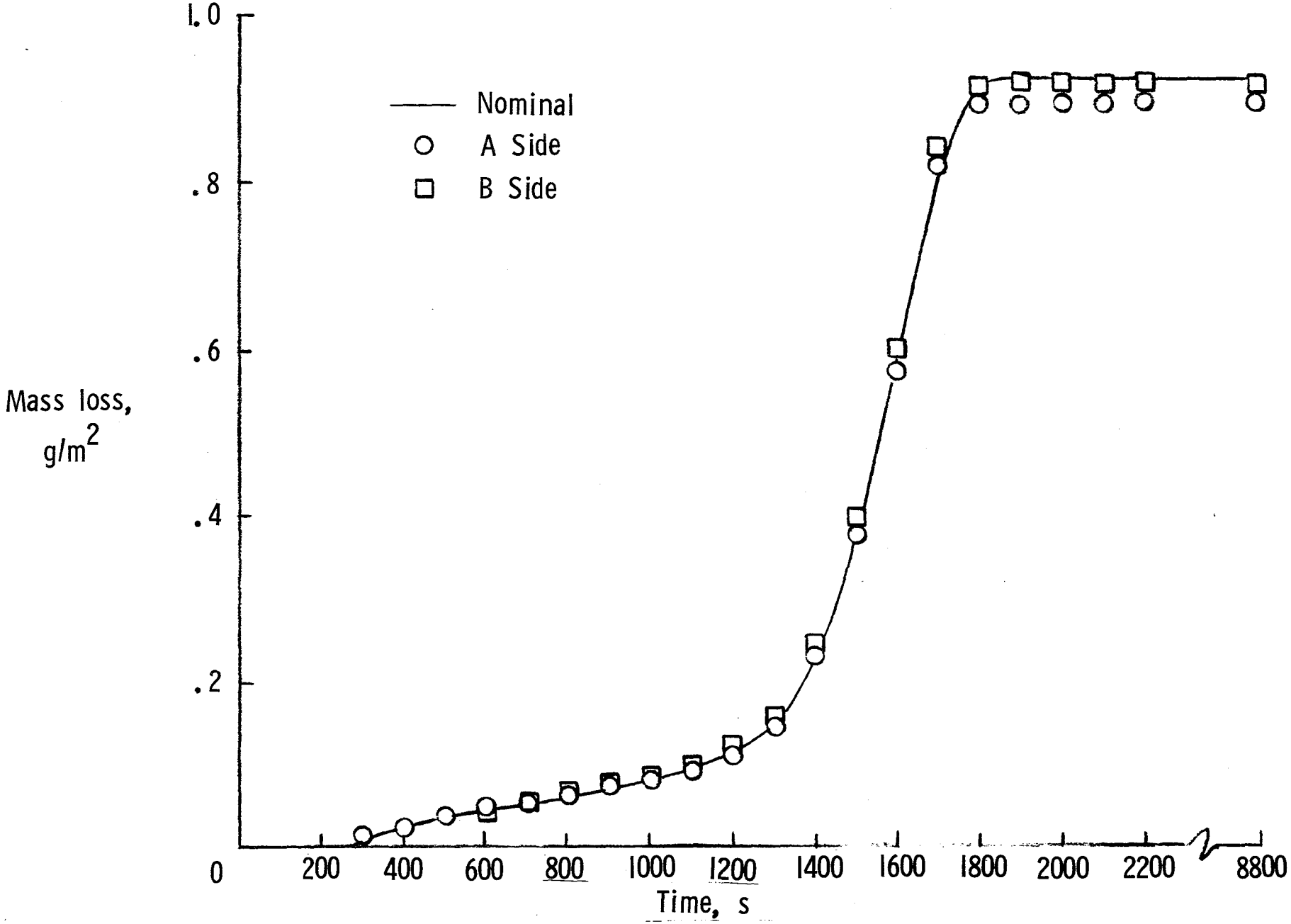

Figure 15.- Calculated mass loss at positions A and B for typical calibration mission using measured specimen temperatures and chamber pressure.

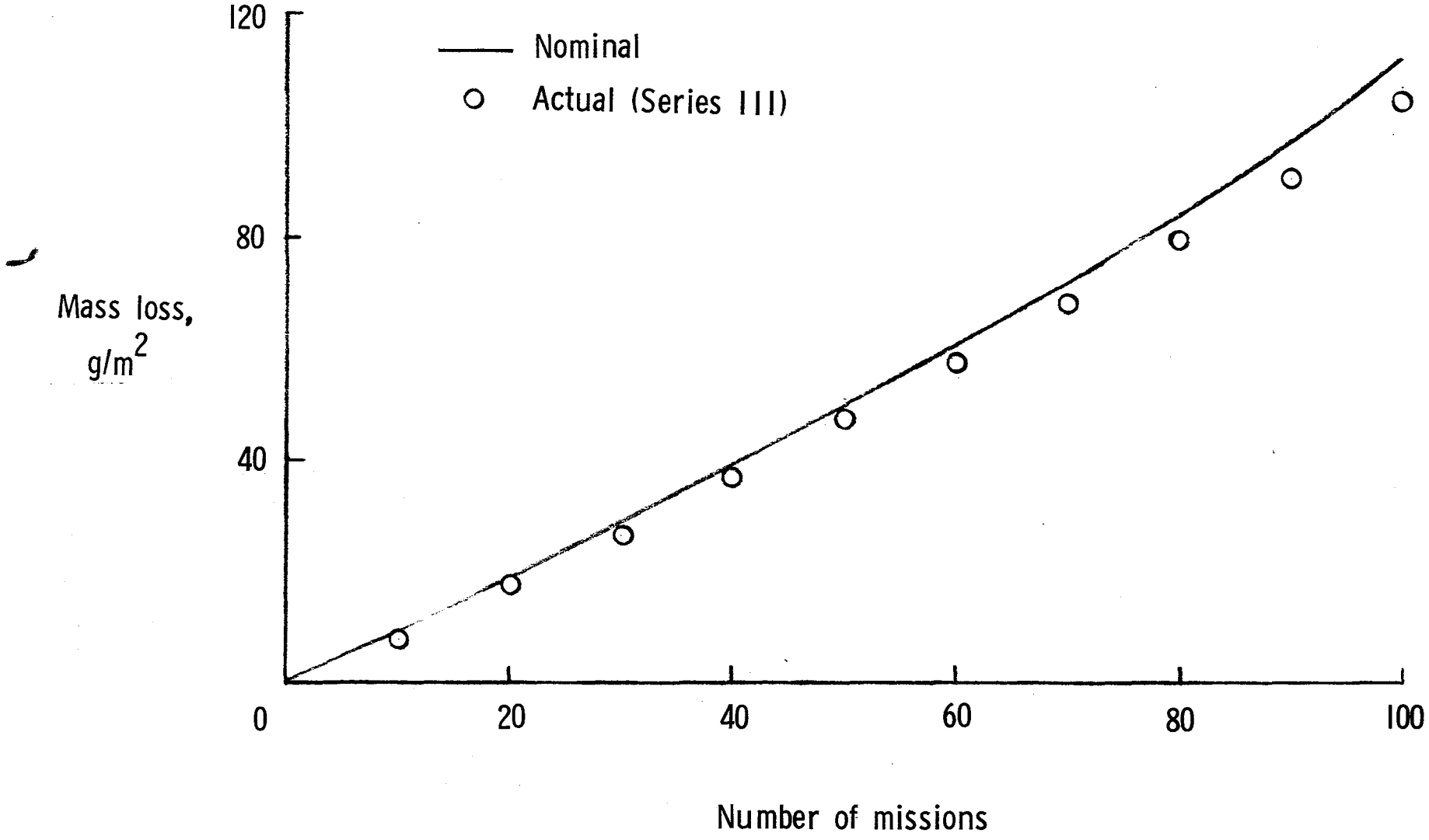

Figure 16.- Comparison of calculated mass loss for nominal and actual mission profiles.

1. Report No.	2. Government Accession No.	3. Recipient's Catalog No.
NASA TM- 83203		

4. Title and Subtitle	5. Report Date
MASS LOSS OF TEOS-COATED RCC SUBJECTED TO THE ENVIRONMENT AT THE SHUTTLE WING LEADING EDGE	September 1981
	6. Performing Organization Code 505-33-23-03

7. Author(s)	8. Performing Organization Report No.
C. W. Stroud and Donald R. Rummler	
	10. Work Unit No.
9. Performing Organization Name and Address NASA Langley Research Center Hampton, VA 23665	11. Contract or Grant No.
	13. Type of Report and Period Covered Technical Memorandum
12. Sponsoring Agency Name and Address National Aeronautics and Space Administration Washington, DC 20546	14. Sponsoring Agency Code

15. Supplementary Notes

16. Abstract

Coated, reinforced carbon-carbon (RCC) is used for the leading edges of the Space Shuttle. The mass loss characteristics of RCC specimens coated with tetra-ethyl-ortho-silicate (TEOS) were determined for conditions which simulated the entry environment expected at the stagnation area of the wing leading edge. Maximum specimen temperature was 1632 K. Specimens were exposed for up to 100 missions. Stress levels up to 8.274 MPa caused an average increase in oxidation of 6 percent over unstressed specimens. Experimentally determined mass losses were compared with those predicted by an existing empirical analysis.

17. Key Words (Suggested by Author(s))	18. Distribution Statement
Mass Loss Tetra-ethyl-ortho-silicate (TEOS) Oxidation Reinforced Carbon-carbon Composites (RCC)	Unclassified-Unlimited Subject Category 24

19. Security Classif. (of this report)	20. Security Classif. (of this page)	21. No. of Pages	22. Price*
Unclassified	Unclassified	58	A04

For sale by the National Technical Information Service, Springfield, Virginia 22161